Distribution and characteristics of supraglacial channels on mountain glaciers in Valais, Switzerland

Holly Wytiahlowsky[1], Chris R. Stokes[1], Rebecca A. Hodge[1], Caroline C. Clason[1], Stewart S.R. Jamieson[1]

[1]Department of Geography, Durham University, Durham, DH1 3LE, United Kingdom

Correspondence to: Holly Wytiahlowsky (holly.e.wytiahlowsky@durham.ac.uk)

Abstract. Supraglacial channels form a key component of glacier hydrology, transporting surface meltwater to englacial and proglacial positions, which impacts ice flow dynamics, surface mass balance and the hydrochemistry of glacial runoff. The presence of supraglacial channels is well-documented on ice sheets using satellite imagery, but ~~little~~much less is known about their ~~distribution and characteristics~~properties on mountain glaciers ~~because most channels fall below the resolution of freely-available satellite imagery.~~. Here we use high-resolution (0.~~15~~1 m) orthophotos to identify channels across 285 glaciers in Valais Canton, Switzerland. For the 85 glaciers with visible supraglacial ~~channels (>0.5 m wide),~~drainage networks, we ~~mapped~~map 1890 channels (> 0.5 m wide) and investigate their distribution and characteristics. We find ~~that~~ glacier hypsometry, size, and slope are good predictors of drainage density, with glaciers characterised by ~~lower angle~~shallow slopes (which have fewer crevasses) and larger ~~ablation~~snow-free areas (with a high meltwater supply) exhibiting higher drainage densities. The strongest control on drainage density is mean glacier ~~mean~~elevation, with glaciers ~~containing a larger portion of their mass~~ at lower elevations producing higher drainage densities. On average, 80 % of ~~high order~~ channels ~~run off supraglacially~~drain across the glacier and directly onto proglacial areas, with 20 % terminating englacially. However, there is ~~marked~~large inter-glacier variability ~~in where channels terminate~~, with 40 % of glaciers containing no englacially-terminating channels~~, versus~~ and 3.5 % where all channels terminate englacially. Most channels on glaciers in Valais are slightly sinuous, with higher sinuosities typically occurring in flatter areas and associated with ~~large, high order channels that are heavily incised and more likely to reactivate annually. This differs to an ice sheet setting where many supraglacial channels terminate in lakes and fewer channels reach the ice margin~~patchy debris cover. Future research should assess the importance of channels below our mapping resolution and network evolution under climate change.

1   Introduction

Glaciers and ice caps are ~~rapidly~~ losing mass rapidly (Wouters et al., 2019; Hugonnet et al., 2021; Tepes et al., 2021; The GlaMBIE Team, 2025~~)~~), resulting in sea level rise, which is anticipated to continue throughout the 21st century and beyond (Bamber et al., 2019; Edwards et al., 2021; Rounce et al., 2023). Glaciers in the lower latitudes (e.g., the European Alps, Caucasus, New Zealand, the USA) are particularly vulnerable to atmospheric warming and may experience complete deglaciation by 2100 under a strong warming scenario (e.g., RCP8.5) (Zekollari et

35 al., 2019; Rounce et al., 2023). In populated mountain regions, these changes will have profound impacts, as

36 glaciers and snowpacks act as vital water towers, supplying freshwater to the 1.9 billion people worldwide who

37 live in or downstream of glacial catchments ~~with crucial freshwater~~ (Carey et al., 2017; Zemp et al., 2019;

38 Immerzeel et al., 2020; Sommer et al., 2020; Hugonnet et al., 2021; Clason et al., 2023). Glacier meltwater

39 ~~responsible for feeding~~that feeds proglacial rivers is commonly transported to the proglacial margin by

40 supraglacial channels, ~~with these channels forming~~which are an important component of the glacial hydrological

41 system. The presence and distribution of supraglacial channels ~~has~~have implications for a range of glacio-

42 hydrological processes as they affect how efficiently meltwater is routed over, through and under glaciers, ~~with~~

43 ~~the potential to impact on~~and can also affect suspended sediment concentrations and hydrochemistry of proglacial

44 rivers. Higher suspended sediment concentrations~~, for example,~~ pose harm to downstream ecosystems and

45 proglacial reservoirs, with concentrations generally higher if meltwater is routed ~~to~~via the bed (Swift et al., 2002),

46 rather than transported ~~supraglacially. In addition,~~across the glacier surface. The presence or absence of channels

47 that route meltwater to the bed ~~directly~~also affects the supply of subglacial meltwater ~~supply~~, which has

48 implications for subglacial water pressure, the onset of subglacial channelisation~~,~~ and ~~could in turn influence~~,

49 potentially, ice motion (e.g., Willis, 1995; Jobard and Dzikowski, 2006; Banwell et al., 2016). Despite the

50 importance of meltwater routing, the controls and patterns of meltwater transport on mountain glaciers remain

51 relatively understudied~~.~~ compared to, for example, the Greenland Ice Sheet (GrIS). Notably, it is not yet fully

52 understood why the channelised flow of meltwater occurs on some glaciers but not others (Pitcher ~~&~~and Smith,

53 2019).

54 The term 'supraglacial stream' was first coined in the 1970s and 1980s from observations of channels in

55 Scandinavia and the European Alps (e.g., Knighton, 1972, 1981, 1985; Ferguson, 1973; Hambrey, 1977; Seaberg,

56 1988), with their morphology (i.e., channel shape and structure) often compared to terrestrial streams. However,

57 these early studies only provided small-scale, local observations of channels on individual glaciers. By

58 comparison, a recent revival in supraglacial channel research has primarily focused on large-scale remote-sensing

59 observations of the ~~Greenland Ice Sheet (~~GrIS~~)~~ (e.g., Smith et al., 2015; Karlstrom and Yang, 2016; Gleason et

60 al., 2021; ~~Karlstrom & Yang, 2016;~~Yang et al., 2015, 2016, 2018, 2019, 2020, 2021, 2022), and to a lesser extent,

61 Antarctica (e.g., ~~Kingslake~~Bell et al., 2017~~, Bell~~; Kingslake et al., 2017; Chen et al., 2024). Recent remote sensing

62 techniques for channel detection on the GrIS (e.g., Yang and Smith, 2013; King et al., 2016) have ~~not~~rarely been

63 applied to mountain environments ~~because the majority of~~, as most channels on mountain glaciers are likely ~~to~~

64 ~~be~~much smaller and therefore fall below the resolution of even the highest~~-~~-resolution freely available satellite

65 platforms (e.g., Sentinel-2~~ (~ 10 m), WorldView 3 (0.31 and 1.24 m))~~., ~10 m). As a result, it is not known whether

66 the ~~principles that govern channel formation on larger~~characteristics of channels on ice sheets ~~also apply~~and the

67 controls on their distribution are comparable to channels on mountain glaciers. The latter are characterised by less

68 available space for channel formation, tend to have a larger debris coverage, and typically contain steeper and

69 more complex topography ~~and tend to have a larger coverage of debris cover in comparison~~compared to ice sheet

70 surfaces.

71 ~~Much~~Whilst much remains unknown about supraglacial channel distribution in mountainous environments, ~~but~~

72 previous research has ~~helped to establish~~established some ~~fundamentals~~fundamental principles (e.g., Knighton,

73 1972, 1981; Ferguson, 1973; Yang et al., 2016). ~~Specifically, the~~The formation of ~~meltwater~~supraglacial channels

74 is thought to occur when channel incision via thermal erosion exceeds the rate of surface lowering (Marston,

75 1983). Channel formation is also influenced by the rate of meltwater production and surface topography, with

76 channels tending to form parallel to the steepest ice flow direction (Irvine-Fynn et al., 2011; Mantelli et al., 2015).

77 Surface topography may ~~re enforce~~reinforce itself, as once an incised channel forms, the higher incision rates may

78 result in an increasingly topographically constrained channel that reactivates annually. ~~On~~At a smaller scale, ~~high~~

79 ~~concentrations of channels~~ micro- to macro-scale surface structures have been suggested to influence meltwater

80 routing (Irvine-Fynn et al., 2011), while high supraglacial channel density appears to be correlated with ~~high, and~~

81 may contribute to, increased surface roughness (~~Irvine-Fynn, 2011), while the presence of micro to macro scale~~

82 ~~surface structures also influences meltwater routing (e.g.,~~ Rippin et al., 2015). Where channels occur, they are

83 often reactivated annually depending on their depth, with the most deeply incised channels suggested to be a

84 product of high discharge or high slope (St Germain ~~&~~and Moorman, 2019). However, incised channel profiles

85 are not typically uniform, and most channels commonly exhibit asymmetric cross-profiles due to the dominant

86 direction of solar radiation (St Germain ~~&~~and Moorman, 2019). Additionally, discharge ~~rates are~~is a strong control

87 on channel ~~morphology, in particular~~form, especially sinuosity, with channels observed to increase in sinuosity

88 throughout the melt season (e.g., Dozier, 1976; Hambrey, 1977; St Germain ~~&~~and Moorman, 2019). Similar to

89 terrestrial river networks, supraglacial channels generally follow Horton's laws, meaning that higher-order

90 channels (i.e., where the highest-order is the main channel) are longer, have lower slopes, and are comprised of a

91 lower number of channel segments (Horton, 1945; Yang et al., 2016). However, much of what we know about

92 supraglacial channels was established from cold to polythermal glaciers or from observations of a small number

93 of individual glaciers (e.g., Knighton, 1972, 1981, 1985; Gleason et al., 2016; St Germain ~~&~~and Moorman, 2019).

94 In this paper, we investigate a range of potential controls on channel distribution and properties for a large sample

95 of glaciers (n = 285) in a region characterised by high melt rates. We use high-resolution (~0.~~15~~1 m) orthophoto

96 imagery from 2020 to produce the first comprehensive inventory of 1,890 supraglacial channels in a mountain

97 glacier environment, with a focus on Valais Canton, Switzerland. Our aim is to characterise the morphometry (i.e.,

98 quantitative measurements of channel geometry) of supraglacial channels on mountain glaciers, providing insight

99 into where and why they form. This is important for understanding how mass is transported through and away

100 from ~~glacier~~glaciers, and for determining ~~how uniform~~ the extent to which surface hydrological characteristics

101 (e.g., channel~~, channel~~ transport pathways) are uniform between glaciers, which is beneficial for informing

102 modelling of glacier hydrology and ice motion. Using GIS software, we extract channel metrics (length, sinuosity,

103 slope, elevation, terminus type, proximity to debris) and glacier characteristics (aspect, size, drainage density,

104 elevation, crevassed extent~~)~~), which are supplemented by qualitative observations. ~~Using our data, we~~We then

105 explore the relationship between glacier and channel characteristics using statistical measures and infer whether

106 glacier surface characteristics can explain the presence or absence of channels.

2   Study location

109 ~~When compared~~Compared to many glacierised regions, Switzerland has the largest repository of high spatial and

110 temporal resolution national LiDAR and orthophoto surveys, providing excellent coverage for the mapping of

111 supraglacial channels. We focus on Valais Canton in southern Switzerland, which contains 303 glaciers over 0.1

km², covering a total area of 545 km² in 2015 (Fig. 1; Linsbauer et al., 2021). It is the most glacierised Swiss Canton, and in 2015, glaciers in Valais had a mean area of 1.8 km², a median of 0.43 km² and a maximum area of 77.3 km² (Grosser Aletschgletscher) (Linsbauer et al., 2021). We identified Valais Canton as a suitable study site as its glacier size distribution is comparable with ~~Switzerland~~Switzerland's as a whole, and the glaciers range from shallow to steep gradients, have differing hypsometries (ice area-elevation distributions~~)~~), and ~~vary in~~varying crevasse densities. Thus, this study site captures a wide range of potential influences on channel distributions and characteristics. Valais is comprised of the Bernese Alps to the north and the Pennine Alps in the south, separated by the Rhône Valley (Fig. 1). Glaciers in the Bernese Alps are the largest in the canton and most exhibit a south-to-southeast aspect (mean: 163°). In contrast, the largest glaciers in the Pennine Alps have a north and west aspect (mean: 347°). Glaciers in Valais have an average maximum elevation of 3450 m.a.s.l (min: 2356, max: 4599) and an overall mean elevation of 3091 m.a.s.l (min: 2267, max: 4025).
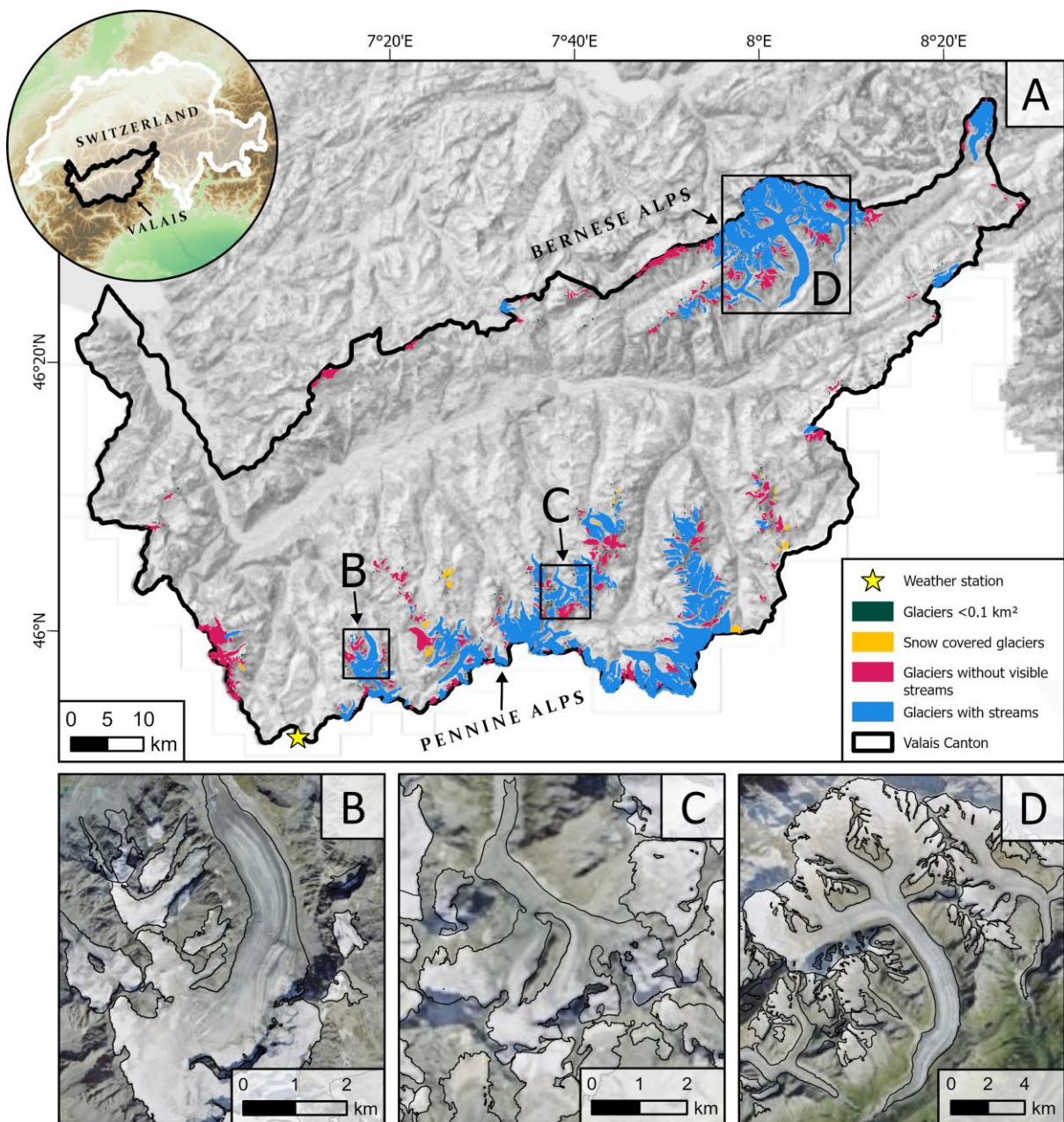
Figure 1: The study site area, which contains 303 glaciers > 0.1 km². (A) The location of Valais Canton (black) is shown within southwest Switzerland. Glaciers ~~found to contain~~containing visible streams (> 0.5 m wide) are shown in blue, glaciers without visible streams ~~(>0. 5 m wide)~~ are in pink, glaciers fully covered by snow are in yellow, and all glaciers < 0.1 km² (which we omit from this study) are shown in dark green; (B) an example of a large valley glacier~~,~~ (Glacier de Corbassière), with smaller glaciers at higher elevations; (C) the debris-covered tongue of Glacier du Grand Cornier and surrounding smaller glaciers; and (D) the larger glaciers (e.g., Grosser Aletschgletscher, centre right) in the north of Valais ~~Canton~~. The location of Col du Grand St-Bernard meteorological weather station is indicated by a yellow star. Glacier outlines used are from the Swiss Glacier Inventory (SGI2016), with glacier extent shown for 2015-16. The outlines are overlayed on basemap imagery sourced from Esri (2024).

Within Valais, the only meteorological station with a similar elevation to many glacier termini is Col du Grand St-Bernard (2472 m.a.s.l) in the Pennine Alps~~,~~ (Fig. 1), which (between 1991 and 2020) recorded mean July air temperatures (2 m) of 8.4 °C, mean January temperatures of -6.9 °C, and mean annual temperatures of -0.1 °C. At Col du Grand St-Bernard, July averages 140 mm of precipitation (1991-2020), with 12.7 days a month experiencing > 1 mm of precipitation, compared to a January average of 242 mm across an average of 12.9 days. However, Switzerland's climate is changing and mean air temperatures between 2013 and 2022 were 2.5 °C warmer than pre-industrial temperatures (MeteoSwiss, 2024), which has greatly impacted the mass balance of Swiss glaciers in recent decades (Fischer et al., 2015; Davaze et al., 2020).

3 Methods

3.1 Imagery acquisition and channel delineation

The method commonly used for automated channel detection, developed by Yang and Smith (2013) for delineating water bodies on the GrIS from WorldView-2 imagery (1.84 m), ~~involves the application of~~uses a normalised difference water index adapted for ice (NDWI$_{ice}$). Following Yang and Smith (2013), we applied a modified NDWI$_{ice}$ approach to a high-~~-~~resolution (0.~~15~~1 m) orthophoto tile (1 km by 1 km) on the Grosser Aletschgletscher. However, our NDWI$_{ice}$ output predominantly detected water-filled crevasses, and whilst it was able to detect some channels > 0.5 m in width, it typically identified only the largest channels (mostly > 1 m). It also missed many channels that were visible but contained very small amounts of water, or incised channels where the water surface was not visible. This method is likely better suited to coarser imagery (less visible crevasses) in less complex terrain and/or for simply using a threshold to extract ~~high ~~higher-order channels. As a result, we undertook manual mapping, which in some instances ~~has been found to be seven fold~~is sevenfold more accurate in ascertaining channel density compared to automated methods (King et al., 2016).

We obtained high-resolution cloud-free orthophoto imagery (0.~~15~~10 m resolution) from SwissTopo (swisstopo.admin.ch), with acquisition dates during mid-July 2020. Imagery was not available for later in the melt season~~. Hence,~~ which lasted from approximately April to September 2020 at Col du Grant St Bernard. Hence, our data is unlikely to capture the peak extent of channel distribution, which is expected to occur in late summer.

161 Snow conditions at Col du Grand St~~--~~Bernard ~~(Fig. 1)~~ in mid-July ~~2020~~ were likely to be lower than average ~~(2010~~

162 ~~to 2020 mean~~, as the precipitation of the preceding winter (total~~: 704 mm) due to low total winter (~~ across

163 December, January, February) ~~precipitation in 2019/20 (2019/20 total: 570 mm). However,~~ was 570 mm compared

164 to the 2010 to 2020 mean of 704 mm. May temperatures were slightly warmer than average (2020 mean: 3.4˚C;

165 2010-20 mean: 1.7˚C), followed by a colder than average June (2020 mean: 4.8 ˚C; 2010-2020 mean: 6.3 ˚C),

166 meaning that whilst there was less snow, it may have melted more slowly than previous years.

167 ~~Our~~We first ~~procedure was to remove~~removed all glaciers in Valais ~~Canton~~ smaller than 0.1 km^2 from our study

168 ~~glaciers~~sample (582 reduced to 303 glaciers). This is because they are likely too small to produce large enough

169 channels to be detected by our imagery, and because many small glaciers in the Swiss Glacier Inventory (SGI2016)

170 are unlikely to meet the criteria to be identifiable as glaciers (Leigh et al., 2019). Due to the date of imagery

171 acquisition, 6 % of the remaining 303 glaciers were still completely snow-covered and were omitted from further

172 analyses as the presence or absence of channels could not be detected, ~~resulting in~~leaving 285 glaciers ~~remaining~~

173 ~~in our sample.~~. Within ~~this sample~~these glaciers, the mean ~~percentage~~ snow-free ~~glacier~~ area was 38.9 % in mid-

174 July 2020, with some variation in snow cover at different elevation bands. For example, glaciers with a mean

175 elevation between 2500 ~~–~~ 2800 m.a.s.l had a 45.0 % snow-free area on average, compared to 36.6 % at 3100 ~~–~~

176 3400 m.a.s.l. The lowest percentage of snow-free area was 4.9 % at a high elevation cirque, and five glaciers were

177 completely snow-free by mid-July but were all under 0.7 km^2.

178 Each glacier was systematically surveyed for supraglacial channels in *QGIS* (e.g., Fig. 2). Of the 285 glaciers that

179 we surveyed, 85 supported supraglacial channels above our mapping threshold. Only channels confidently visible

180 at a 1:1,000 scale were delineated for the purpose of consistency, meaning the minimum channel width we

181 delineated was ~0.5 m ~~wide~~. We solely focus on these larger ~~(>0.5 m)~~ channels because of difficulties in

182 delineating small channels objectively, which include problems with differentiating complex rill networks from

183 structural features (e.g., fractures~~) and the need for more subjective judgments where channel width~~). Additionally,

184 smaller channels may have widths that periodically ~~decrease~~fall below the pixel ~~width~~resolution, which may

185 require subjective judgments to be made. Whilst we do not map channels below the scale defined above, many of

186 the glaciers likely contain smaller channels ~~(< 0.5 m wide)~~ that are not sufficiently clear enough to map. These

187 smaller channels may ~~still~~ form a key hydrological component of these glaciers, but we ~~cannot reliably quantify~~

188 ~~their existence, particularly for smaller glaciers, hence we focus on~~anticipate that the channels ~~>0.5 m wide, which~~

189 ~~are also likely to~~we have mapped carry the bulk of the meltwater. Individual channels were mapped from their

190 downstream end until they were no longer clearly visible or when channels could not be confidently and

191 objectively mapped. When channels have tributaries above the mapping resolution, the main channels ~~were~~are

192 mapped as one segment, continuing up the largest channel at each confluence. Each tributary channel was then

193 subsequently mapped as a new individual segment. Once mapped, each entire channel segment was assigned

194 ~~codes~~a code based on its attributes and whether it was on ~~a~~ bare ice, surrounded by patchy debris, or on a debris-

195 covered part of the glacier. The ~~location~~type of ~~the channel~~ terminus was assigned ~~for~~to each channel, which

196 ~~includes the following categories:~~was one of: running off the glacier terminus, terminating in a moulin, crevasse,

197 lake, the glacier periphery, adjoins another channel, ~~and~~or disappears beyond the resolution (i.e., the terminus is

198 not visible and cannot be confidently inferred).
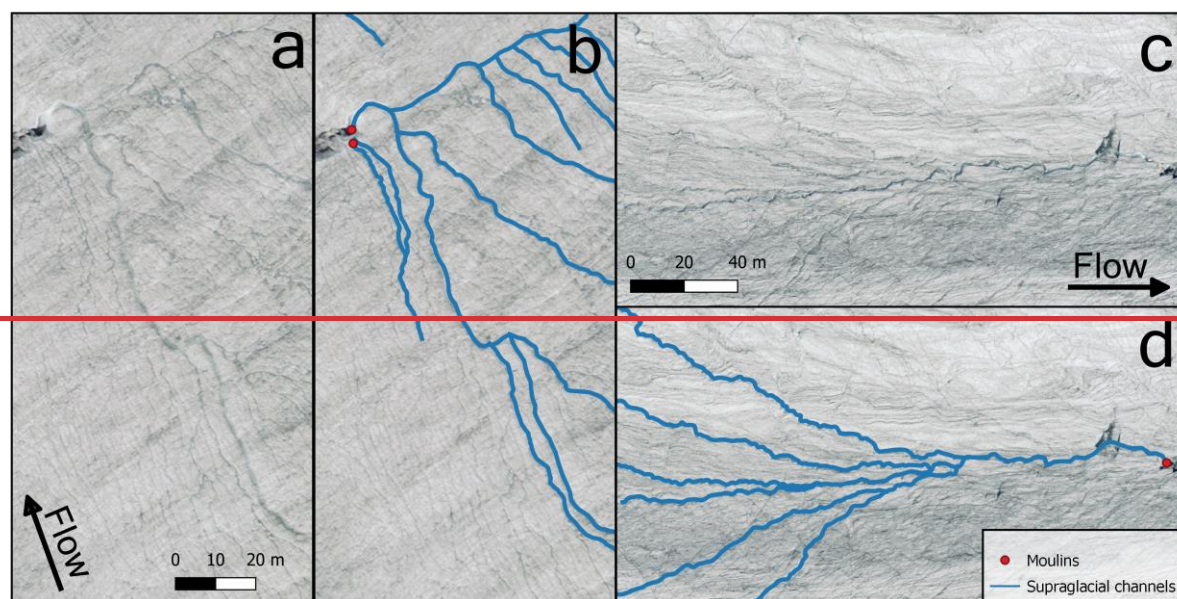
Figure 2: Examples of the mapped output and corresponding orthophoto. Channels are shown in blue, and moulins are represented ~~as~~by red circles when a mapped channel is moulin-terminating. Arrows indicate the direction of ice flow. (a—b) Supraglacial channels on the Glacier de Moiry and (c-d) Allalingletscher. Imagery source: Federal Office of Topography ~~swisstopo~~Swisstopo.

To ensure consistency, all mapping and the error assessment ~~was~~were conducted by the same individual. We quantified the repeatability of our mapping by delineating channels from the same image of the Rhonegletscher ~~independently~~on two occasions, months apart. This revealed a 2.6 % difference in calculated drainage density and a 0.21 % decrease in total channel length from the original mapping (Figure ~~S3~~B1). The error from our repeat mapping may have been lower if the mapping ~~has~~had been repeated immediately after the original mapping, whereas the original mapping was conducted consistently over a time period. However, the error margin is small enough for us to ~~provide~~conclude that the original mapping provided a good representation of each glacier's

212 drainage density. Both sets of mapping also clearly ~~identify~~identified where channels terminate~~, but the~~. The
213 primary source of uncertainty here stems from ~~determining~~knowing when to stop mapping up-channel~~.~~ and total
214 channel length. We therefore ~~take~~took a conservative approach to avoid over-interpreting channel pathways and
215 only ~~map~~mapped the up-glacier limit of channels where we are confident that it exists.

3.2   Metrics

A total of 1890 channel segments (polylines) were mapped across ~~85~~the glaciers ~~found to contain~~that contained channels. We then used the high-resolution (0.5 m) SwissALTI3D DEM (2019) from swisstopo.admin.ch (1 sigma accuracy of ± 0.3 m for each dimension) to extract morphometric characteristics from each channel segment. The DEM is coarser than the orthophotos used for channel delineation, and there is a one-year offset between their acquisition dates. However, as the DEM is used to calculate larger-scale metrics such as elevation and slope, the small offset is unlikely to affect overall results. ~~Channel~~Extracted channel metrics ~~extracted~~ were segment length, straight line distance, elevation (minimum, maximum), elevation difference, and channel slope. The start and end ~~point~~points of each segment were then used to derive the sinuosity of each segment (channel length/straight line distance) and drainage density for each glacier (total length of channels/glacier area). We ~~use~~used the glacier snow-free area at the time of mapping to calculate drainage density, which ~~results~~resulted in a higher value ~~that~~than if the entire glacier area ~~was~~had been used.

Glacier characteristics were obtained from the Swiss Glacier Inventory (SGI2016), which ~~provided information on~~included glacier area, aspect, and elevation (minimum, maximum and mean) in 2015 (Linsbauer et al., 2021). This record is ~~used as it is~~ the most up-to-date record of Swiss glacier area, but glaciers have since undergone substantial recession. ~~The~~Glacier slope values ~~for glacier slope~~ from the SGI2016 cannot be used as they encompass the whole glacier, whereas for our analysis, we wanted to measure the slope of the snow-free portion of the ablation area at the time of channel mapping. To calculate slope values, each glacier polygon was clipped to its snow-free area, and then zonal statistics in *QGIS* were used to extract the mean, minimum and maximum slope value from the SwissALTI3D DEM for each polygon. The snow-free slope value is the only glacial slope value used in data analyses. ~~Upon completion of mapping, we~~We assigned codes to each glacier based on the ~~extent~~size of ~~debris cover and~~the crevassed area due to ~~their~~its potential ~~controls~~impact on channel formation. ~~Glacier debris cover is visually estimated and allocated to one of five~~This included the following classes ~~(none, <10%, 10-25%, 25-50% and >50%) and crevassed area is assigned to one of three classes~~: little to ~~none~~no (less than 10 % of the ~~ablation~~snow-free area), moderate (10-50 % covered), and heavily crevassed (covers > 50 % of the ~~ablation~~snow-free area).

3.3   Statistical tests

To determine whether there is a relationship between channel morphometry and glacier characteristics, we produced a correlation matrix using Spearman's rank correlation (ρ) (e.g., St Germain ~~&~~and Moorman, 2019). Each metric used in this analysis comprises 1890 values, each representing an individual channel segment. The analysis used the following channel variables: segment length, channel slope, sinuosity, minimum elevation,

249 maximum elevation and elevation range, and the following glacier variables: drainage density, glacier area, mean

250 slope of the snow-free area, aspect, glacier minimum elevation, glacier mean elevation, and glacier maximum

251 elevation. For each of the glacier variables, all channel segments on the same glacier ~~are~~were allocated the same

252 value. A singular ANOVA test was conducted to determine the significance of the relationship between debris

253 cover and sinuosity, as an ANOVA test is best suited to determining if there is a significant difference between

254 different classes of debris cover. We also conducted a Principal Component Analysis (PCA) to determine the

255 relationship between variables and to identify drivers of variance amongst the dataset, with data normalised to aid

256 in identifying patterns within the data.

257

4 Results

258 **4   Results**

259 **4.1   Glacier observations**

260 ~~The study area contained 285 glaciers with an area over 0.1 km² and a snow-free terminus in 2020 (Linsbauer et~~

261 ~~al., 2021). Of these, 85 glaciers were found to have supraglacial channels above the mapping resolution (~0.5 m).~~

262 Glaciers with channels (n = 85) have a larger mean area ~~of 5 km² and~~than glaciers without ~~visible large~~ channels

263 ~~(>0.5 m)~~ (n = 200) ~~have a (~~mean area ~~of~~= 5 km² vs. 0.6 km². ~~However, glacier area frequency distributions peak~~

264 ~~in the 0.1 to 1 km² category for both glaciers with and without visible channels (Fig.~~) and all~~3a). All~~ glaciers

265 larger than 5.6 km² ~~were found to~~ contain channels > 0.5 m wide (Table 1, Fig. 3a). However, the modal glacier

266 area is 0.1 to 1 km² for glaciers both with and without visible channels (Fig. 3a). ~~Where channels are present,~~

267 ~~glaciers have an overall mean slope of 21° and a maximum mean slope of 43°, with glacier slope being positively~~

268 ~~skewed towards~~Glaciers containing channels typically have lower ~~slope values (Table 1, Fig. 3b). By comparison,~~

269 ~~where visible channels are absent, glaciers are characterised by steeper overall~~ slopes compared to those without

270 channels (mean slope: 21° vs. 28°) (Fig. 3b). Glaciers with channels generally have longer tongues that terminate

271 at lower elevations (mean minimum elevation = 2797 m vs. 2936 m) and have higher maximum elevations (mean~~:~~

272 ~~28°,~~ max elevation = 3637 m vs. 3555 m). :~~45~~The mean drainage density on glaciers with channels is 2.4 km/km²

273 and a maximum of 15.2 km/km². The latter was found on Oberer Theodulgletscher, which has the lowest glacier

274 slope in the dataset (13°) (Fig. 3c, Fig. 4a).~~3b).~~

275

276

277

278

279

280

281

282

	Channel Length (m)	Channel Slope (°)	Sinuosity	Drainage Density (km/km²)	Mean Glacier Slope (°)	Glacier Area (km²)
Count	1890	1890	1890	85	85	85
Minimum	5.2	0.8	1.0	0	10.4	0.1
Median	152.2	6.3	1.1	1.5	20.6	1.5
Mean	211.7	8.0	1.1	2.4	21.0	5.0
Maximum	4314.4	47.8	3.8	15.3	43.0	83.0
Range	4309.3	47.0	2.8	15.2	32.6	82.9
Standard Deviation	228.3	6.3	0.1	2.6	6.5	10.7
Standard Error	5.3	0.1	0.0	0.3	0.7	1.2
Kurtosis	65.8	7.4	153.0	9.0	1.1	35.3
Skewness	5.5	2.3	9.5	2.6	0.8	5.4

284 **Table 1: Glacier and channel characteristics.**

285

286

287 ~~Table 1: A quantitative summary of glacier and channel characteristics.~~

288
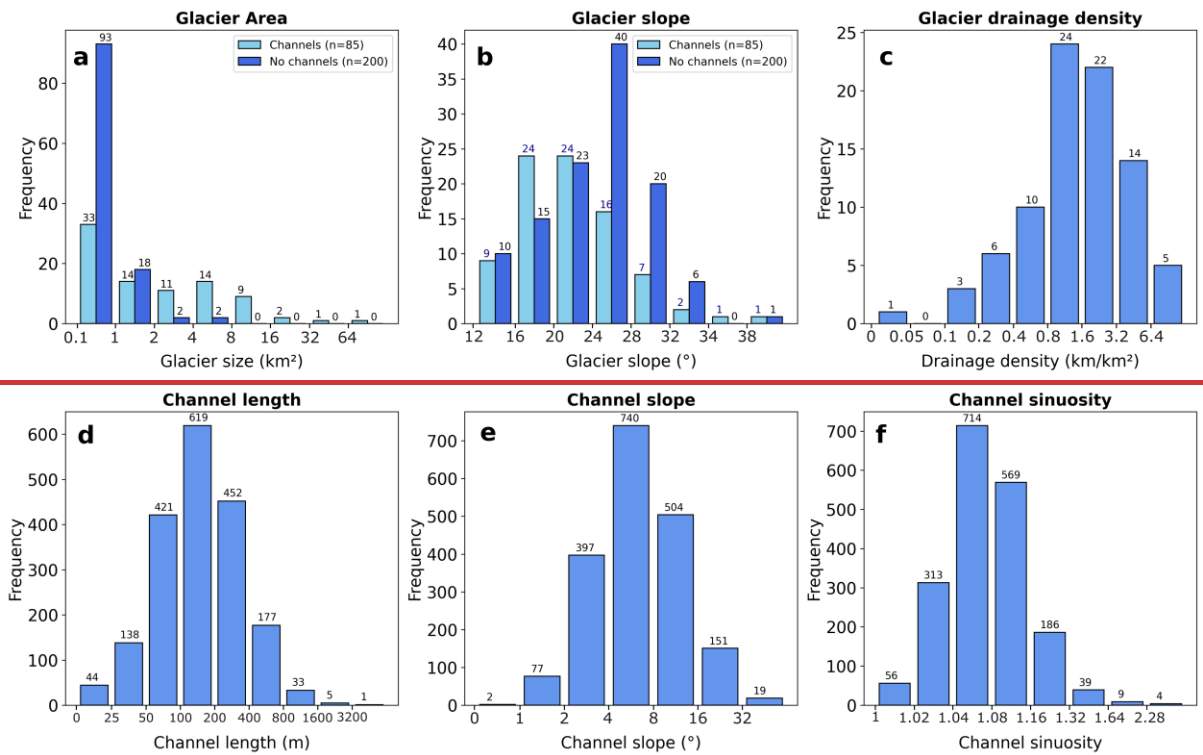
289
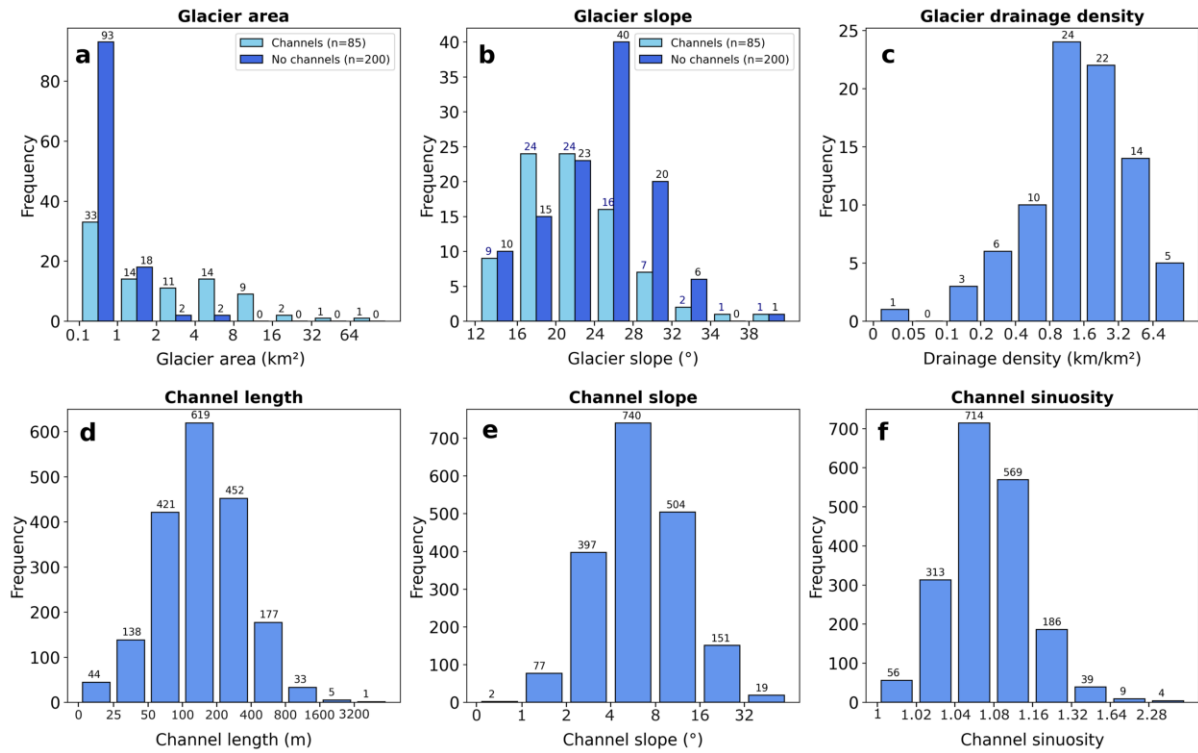
Figure 3: Histograms of extracted metrics. Note that the x-axis ~~is~~uses a log scale (except for Fig. 3b) and the numbers above each bar represent the number of channels/glaciers within each class. The range shown by each bar is indicated by the x-axis values to either side. The range is exclusive of the lower value~~,~~ and ~~include~~inclusive of the higher one (e.g., > 1 - ≤ 2). (a) Glacier area (km²); (b) glacier slope (°); (c) glacier drainage density (km/km²); (d) channel segment length (m); (e) channel slope (°); and (f) channel sinuosity.

297 ~~Glaciers without large channels (>0.5 m) are more likely to terminate at higher elevations (mean minimum~~
298 ~~elevation: 2936 m) compared to glaciers with channels (mean minimum elevation: 2797 m), which are often~~
299 ~~characterised by longer valley glacier tongues. Where glaciers support channels, they are more likely to have a~~
300 ~~higher maximum elevation (mean maximum elevation: 3637 m) than glaciers without large channels (mean~~
301 ~~maximum elevation:~~

302
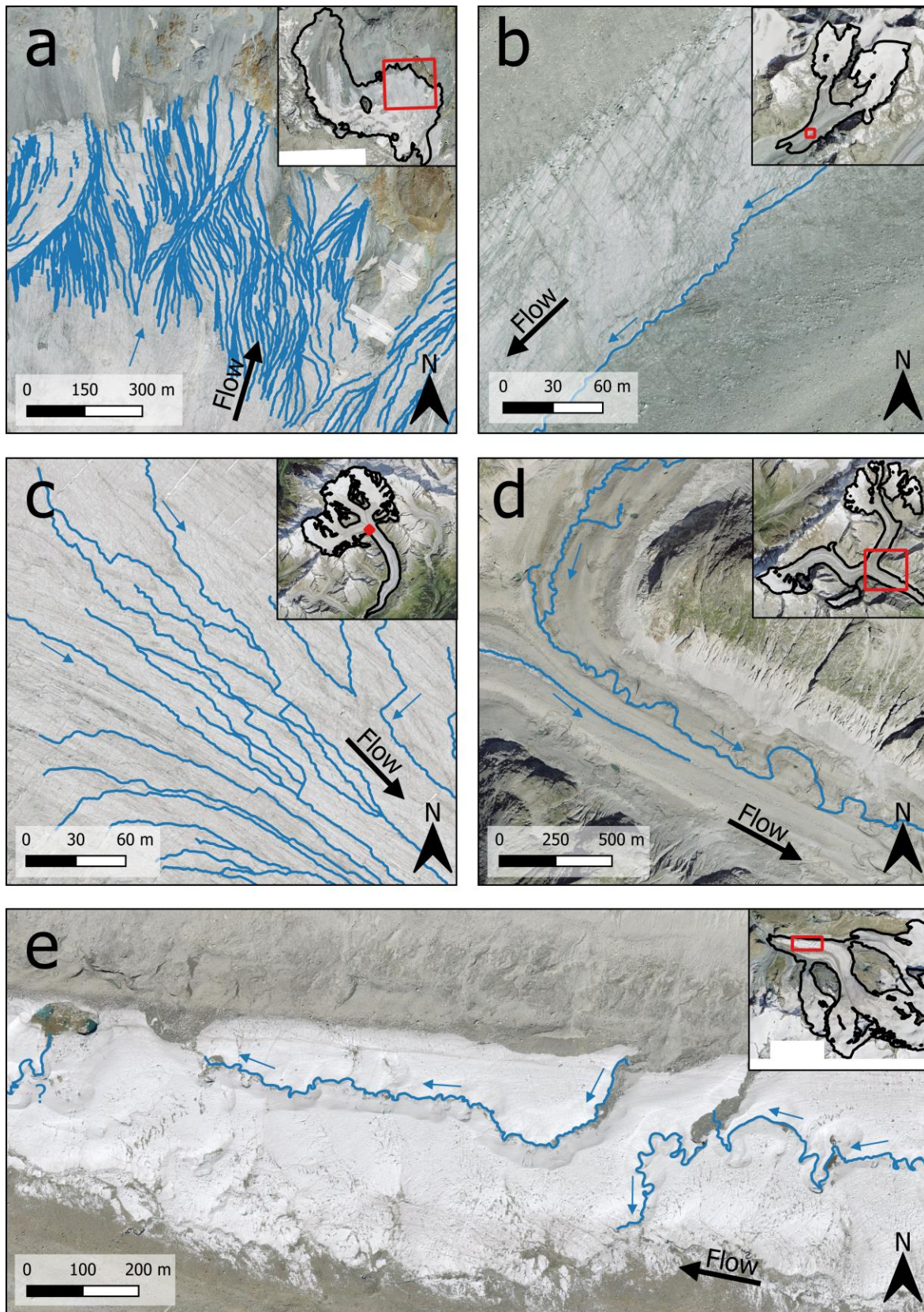
303 ~~3555 m).~~ Where channels >0.5 m are present, there is a mean drainage density of 2.4 km/km² and a maximum of

304 15.2 km/km². The latter was found on the Oberer Theodulgletscher, which is situated on a low slope plateau and

305 has the lowest glacier slope angle in the dataset (13°) (Fig. 3e, Fig. 4a). To summarise, glaciers containing channels

306   are larger, have lower mean slopes, and have a larger portion of their area at lower elevations compared to glaciers
307   without large channels (>0.5 m).
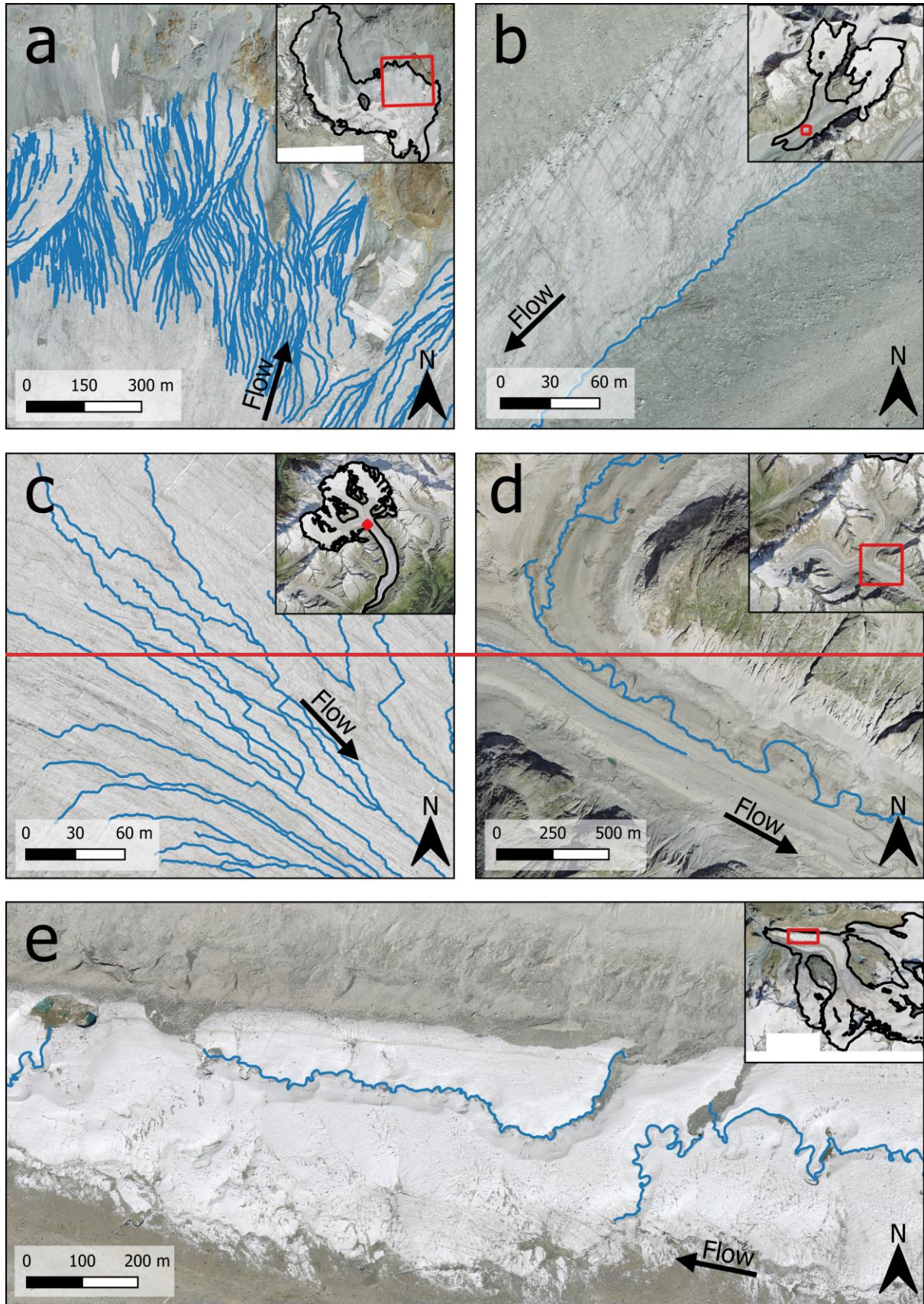
Figure 4: Examples of supraglacial channels. Channel location is shown in relation to the whole glacier in the top ~~left~~right of each panel, with the panel extent shown in red. (a) Channels on the Oberer

Theodulgletscher; (b) a channel at the interface between bare ice and debris-covered ice on Glacier du Brenay; (c) channels on the Grosser Aletschgletscher - note the straight segments where crevasses have been exploited; (d) channels on the debris-covered terminus of the Oberaletschgletscher; and (e) sinuous channels towards the terminus of Gornergletscher, including an example of a ~~channel terminating in a~~ **small supraglacial lake (left).** ~~Flow indicates~~**The black arrows indicate the glacier flow direction**~~.~~**, and the blue arrows indicate the water flow direction. A question mark is shown when the water flow direction is unclear in the DEM. Imagery source: Federal Office of Topography** ~~swisstopo~~**, Swisstopo.**

4.2 Channel characteristics

Individual channel segments have a mean length of 212 m, with a positively skewed leptokurtic distribution (Fig. 3d; Table 1). Few segments exceed 1,600 m, as the ~~length~~snow-free areas of most ~~glacier's ablation area is~~glaciers are smaller than this ~~value~~. The channel segments have a mean slope of 8°, and most exhibit a slope between 4 ~~to~~and 16° (Fig. 3e; Table 1). The maximum channel slope ~~observed~~ is 48°, but the overall distribution is positively skewed towards smaller slope values. The sinuosity index of each channel ranges from 1 (straight line) to a maximum of 3.8, with a mean value of 1.1, which is ~~slightly~~ classified as sinuous~~,~~ (1.05 - 1.25), but not high enough to be defined as meandering (> 1.25) (Table 1) (Brice and Blodgett, 1978). Sinuosity is the most positively skewed variable, with a highly leptokurtic distribution, as most channels are not very sinuous (Fig. 3f).

Channels terminate in a range of settings, with 47 % joining another channel, 15 % terminating in crevasses, 14 % terminating in moulins, 13 % disappearing below the mapping resolution, 8 % running off at the glacier terminus, 2 % running off the side of the glacier, and 1 % terminating in a supraglacial lake (e.g., Fig. 4e). When only considering terminal segments (i.e., channels not adjoining another channel or disappearing below the mapping resolution), 72 % of segments terminate englacially (crevasses or moulins), 25 % run-off (terminus or periphery), and 3 % terminate in a supraglacial lake. However, larger glaciers with higher drainage densities disproportionately impact ~~on~~ these values. For example, 582 out of the 1890 mapped channel segments are on the Grosser Aletschgletscher, where no visible channels reach the terminus~~,~~; hence, englacially terminating channels may be overrepresented by a single glacier. ~~Thus, when~~By comparison, the ~~channel termini locations at each individual~~average glacier ~~are averaged amongst all glaciers with channels > 0.5 m,~~within our dataset is characterised by 80 % of channels ~~reach the terminus supraglacially~~terminating proglacially and 20~~% of channels terminate~~ % terminating englacially. Overall, 48 % of glaciers have no englacially-terminating channels, with only 3.5 % of glaciers ~~that~~ solely ~~contain~~containing englacially terminating channels.

~~Where visible channels occur, qualitative~~Qualitative observations ~~indicate structural and topographic controls on their~~suggest that channel distribution and morphology~~.~~ are controlled by glacier structure and topography. For example, channels often occur ~~at~~along the interface between debris-covered and bare ice (e.g., Fig. 4b), particularly adjacent to medial moraines, where ~~they~~channels are confined to a topographic depression, commonly occurring at the confluence between two tributaries. The influence of glacier structure on channel morphology is also observed where trace or shallow crevasses are exploited to produce long, straight channel sections (e.g., Fig. 4c). By comparison, the most sinuous channels tend to occur at ~~lower~~low elevations on large glaciers characterised by larger flat areas towards to their terminus (Fig. 4e).

349

4.3 ~~Controls on~~ Relationships between channel ~~morphology~~ and ~~distribution~~glacier characteristics

Here, we investigate links between different supraglacial channel and glacier characteristics. Previous studies informed our choice of variables tested for potential relationships, with a focus on how glacier properties (slope, area and elevation) affect glacier drainage density (e.g., Yang et al., 2016) and channel ~~morphology~~morphometry, such as sinuosity and channel segment length (e.g., St Germain ~~&~~and Moorman, 2019). We ~~found~~find that the most sinuous channels are ~~most~~more likely to occur on ~~lower~~shallow slopes (0 to 10°), with ~~an upper boundary demonstrating that~~ channels on steeper slopes (> 20°) ~~are~~ unlikely to exhibit a sinuosity over 1.3 (Fig. 5a). ~~A relationship~~Statistically significant differences in channel sinuosity are also observed between our debris classes (p < 0.05; one-way ANOVA) (Fig. 5c). Channels on patchy ('proximal') debris cover tend to be the most sinuous and are statistically different (p < 0.05; Tukey Honest Significant Difference test) from channels on continuous debris cover ('debris') and those on bare ice ('clean'). The 'debris' class is generally more sinuous than the 'clean' class, but this difference is not statistically significant. Additionally, channel segment length ~~and slope is also apparent, with the longest channel segments occurring on the lowest slope angles (Fig. 5b).~~tends to increase on shallower slopes (Fig. 5b). This relationship is clearly defined by an upper limit, where~~, except for one outlier,~~ channels > 500 m are confined to slopes of < 20˚ and no channels occur on slopes >~~50˚ (Fig. 5b). We find no noticeable difference in sinuosity between channels on bare ice and those on debris covered glaciers~~ 50˚, except for one outlier (Fig. 5b~~5c~~). ~~However, channels proximal to debris (i.e., channels which are likely to have some sediment content) are more likely to be highly sinuous than channels on bare ice or continuous debris cover, with differences between the classes statistically significant (p = <0.05) in an ANOVA test (Fig. 5c).~~ Channel segments that terminate in moulins tend to be the longest (mean: 341 m, max: 1999 m), followed by channels that disappear below the mapping resolution (mean: 259 m, max: 4314 m), and then channels reaching the glacier terminus (mean: 214 m, max: 1193 m) (Fig. 5d). The very few (1 %) channels that terminate in supraglacial lakes tend to be short (mean: 109 m, max: 260 m), as do channels that adjoin a higher-order ~~channels~~channel (mean: 169 m, max: 1174 m) (Fig. 5d).

375
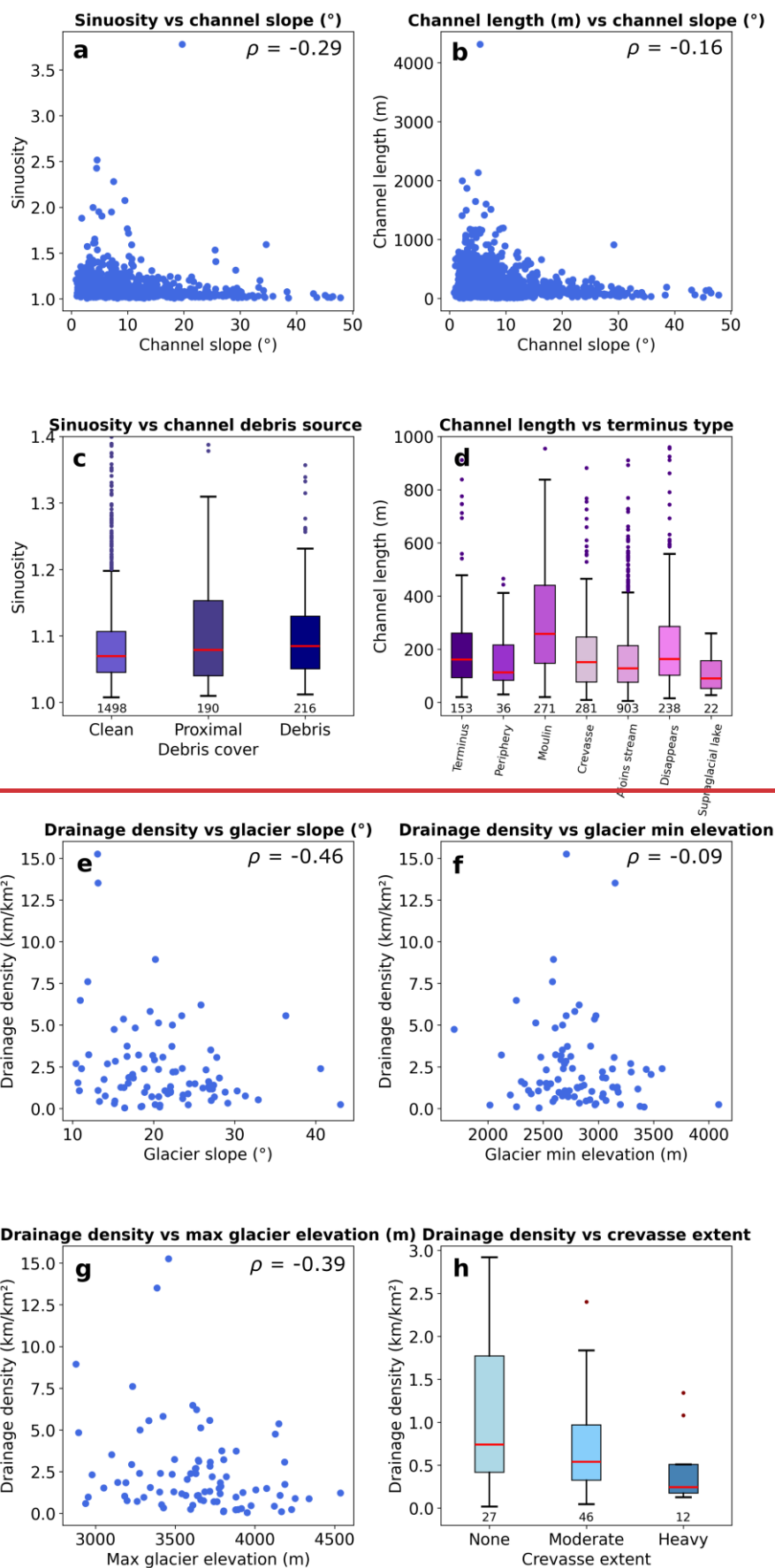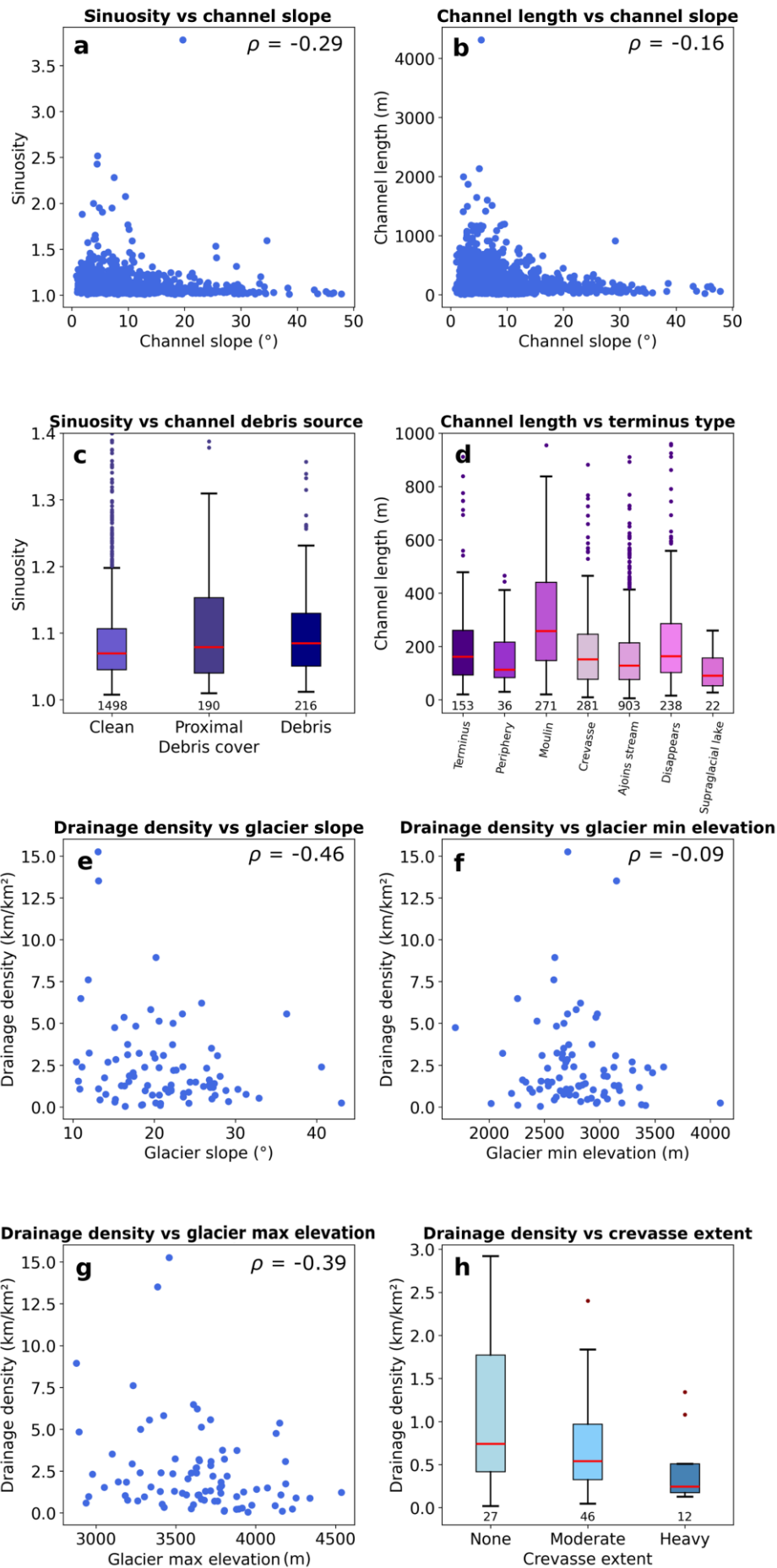
Figure 5: Relationships between channel characteristics (a-d) and glacier metrics (e-h). Plots a-d ~~contains~~contain data from 1890 channels, and plots e-h contain data for the 85 glaciers with visible channels. Spearman's rank (ρ) values are included for all scatterplots, each of which ~~are~~is statistically significant (p ~~=~~< 0.05). (a) Sinuosity vs channel slope (°); (b) channel segment length (m) vs channel slope (°); (c) sinuosity vs channel debris source; (d) channel segment length (m) vs terminus type; (e) drainage density (km/km^2) vs glacier slope (°); (f) drainage density (km/km^2) vs minimum glacier elevation; (g) drainage density (km/km^2) vs maximum glacier elevation ~~(m);~~: and (h) drainage density (km/km^2) vs crevasse extent.

Relationships between glacier metrics (Fig. 5e-h) are less clear than for channel characteristics (Fig. 5a-d), which may be due to the lower number of data points (85 glaciers compared to 1890 channels). However, a moderate negative correlation between drainage density and glacier slope exists, with the highest drainage densities occurring on the lowest surface slopes (Fig. 5e). A relationship between drainage density and minimum glacier elevation is less obvious (Fig. 5f), but there appears to be a peak in drainage density between 2600 and 3100 m.a.s.l, which would require further validation from a larger sample of glaciers. By comparison, there is less evidence of a relationship between glacier drainage density and maximum glacier elevation ~~.~~ (Fig. 5g). Likewise, there is no statistically significant relationship ~~is identified~~ between glacier aspect and drainage density (Kruskal-Wallis test: p = 0.61). ~~Additionally, the crevassed extent of a glacier affects~~Glacier drainage density~~, as increased channel interception prevents the formation of longer channels~~ also tends to be higher on glaciers containing fewer crevasses (Fig. 5h).

4.4   Spearman's rank and ~~principal component analysis~~Principal Component Analysis

We examined the controls on channel ~~morphology~~morphometry and drainage density by calculating a correlation matrix. We use Spearman's rank correlation (ρ) and significance values (p), ~~given that~~as many of our relationships ~~do~~are not ~~appear~~ linear. ~~Additionally, given the~~ Given our large ~~sample size within our~~dataset and the fact that most p-values are ~~< 0~~ 0.05, even modest correlations are statistically significant and likely reflect genuine relationships~~, including weak ones, are significant.~~.

The strongest control on glacier drainage density is ~~identified to be~~ glacier mean elevation (ρ = -0.66, p ~~=~~≤ 0.001), with higher drainage densities ~~present~~observed when a larger portion of glacier ~~mass~~area exists at lower elevations (Fig. 6), followed by glacier mean slope (ρ = -0.46, p ~~=~~≤ 0.001). This is consistent with ~~Fig~~Figure 5e, ~~with~~where the highest drainage densities are observed at glaciers with very low slope angles (e.g., Oberer Theodulgletscher; Fig. 4a).
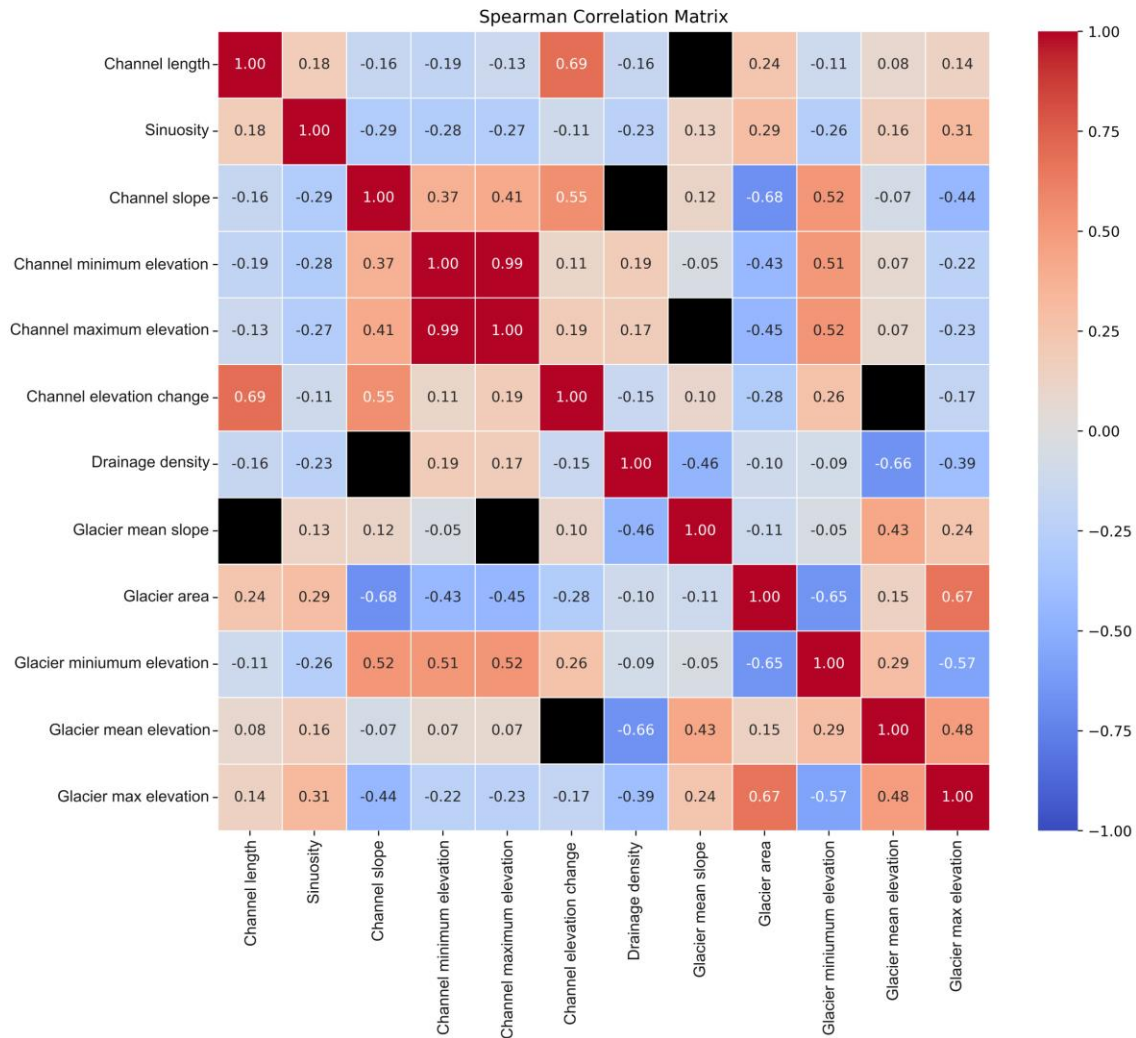
Figure 6: A heatmap matrix of Spearman's rank correlation ~~to show~~showing **the relationship between glacier and channel characteristics. Correlation values are scaled along a colour ramp**, **and non-significant relationships (p**~~)~~ ~~>~~ ≥ **0.05**) **are coloured black.**

By comparison, channel ~~morphology~~morphometry is characterised by more complex and weaker relationships between variables. For example, high channel sinuosity can in part be explained by multiple weak correlations: sinuosity values tend to increase with a decrease in channel slope (ρ = -0.29, p ~~=~~≤ 0.001), and the most sinuous channels occur on larger glaciers (ρ = 0.29, p ~~=~~≤ 0.001) with lower minimum elevations (ρ = -0.26, p ~~=~~≤ 0.001) (Fig. 6). ~~Lower angle surfaces are often found when valley glaciers extend down-valley to flatter terrain, supported by observations of highly sinuous channels on low slope glacier tongues (e.g., Gornergletscher) (Fig.~~ Channel~~4c). The channel~~ slope is primarily controlled by glacier characteristics, with higher slope channels mostly existing on smaller glaciers (ρ = -0.68, p ~~=~~≤ 0.05), which terminate at higher elevations (ρ = 0.52, p ~~=~~≤ 0.05), meaning the steepest channels are likely ~~to be~~ found at high elevation cirques and hanging glaciers.

To assess the relationship between variables and determine the drivers of variance, we conducted a Principal Component Analysis (PCA). The PCA loadings show that glacier area has a large negative loading on ~~principle~~principal component 1, closely followed by strong positive loadings from minimum glacier elevation and channel elevation (maximum and minimum) (Table ~~S1~~A1). By comparison, principal component 2 shows a strong positive loading from drainage density, and large negative loadings from mean glacier slope and glacier mean elevation (Table ~~S1~~A1). The first two components explain 50 % of the variance within the dataset, with an additional 13 %, 12 % and 9 % explained by principal components 3, 4, and 5, respectively, which together explain 84 % of the variability (Table ~~S1~~A1). Given the complexity of the dataset, our ~~cluster~~ analysis reveals no clear visual clustering of data, but the PCA loadings show an expected relationship between elevation variables and slope variables~~, while~~. However, drainage density is not closely related to ~~just one~~any other variable (Fig. ~~S2~~A2). Overall, our PCA analysis reveals no single, primary driver of variance~~,~~; instead, it is apparent that there is a complex, yet interlinked relationship between all variables that explain the distribution and appearance of supraglacial channels.

5   Discussion

5.1   Controls on the spatial distribution of channels

~~Out of~~Of the 285 glaciers ~~examined within~~in our study area, ~~we find that~~ 85 ~~contain visible~~ contained channels (> 0.5 m) ~~using~~visible in high-resolution imagery (0.~~15~~1 m) from mid-July 2020. The presence of visible channels ~~above our mapping threshold (>0.5 m wide)~~ is primarily controlled by a combination of sufficient meltwater supply and distance for meltwater to coalesce and incise. Hence, in ~~mountain glacier environments~~Valais, channels ~~>0.5 m~~ are infrequently detected on cirque glaciers due to their smaller ~~ablation~~snow-free area, steeper and often crevassed slopes, and limited distance for meltwater to coalesce. These cirque glaciers may contain channels below our mapping resolution~~, but these~~; however, they cannot be reliably quantified as part of this study. ~~The glaciers where we observe~~Glaciers containing channels ~~are likely~~tend to be larger, resulting in the production of more surface melt. ~~This is supported by the finding~~We found that all glaciers in Valais larger than 5.6 km^2 supported channels ~~(>0.5 m)~~ and that glacier area controls much of the variability within the dataset (Table ~~S1~~A1), albeit with large variation in drainage density. This variation is in part attributed to glacier slope, which, together with ice flow velocity, governs the crevassed area of a glacier ~~which~~. This crevassed zone, in turn, controls the area in which channels can form. For example, when crevasses are open, they can intercept meltwater ~~which inhibits~~, inhibiting the formation of longer channels~~, whereas~~. Conversely, closed crevasses ~~that have closed~~ can add small-scale variability to surface topography ~~and lead to~~, routing ~~of~~ meltwater along crevasse traces. ~~Additionally, channel~~Channel formation is also governed by glacier hypsometry, with glaciers ~~characterised by~~containing a larger portion of their ~~mass~~area at lower elevations more likely to ~~produce~~have higher drainage densities due to a larger ~~ablation~~snow-free area (Fig. 6). ~~It is assumed~~We assume that ~~we~~our images from mid-July do not capture the maximum channel extent on ~~glaciers with most of their mass at~~ higher ~~elevations due to our imagery acquisition date in mid-July.~~elevation glaciers. However, regardless of the ~~date of imagery~~image acquisition date, channel density will likely remain highest at lower elevations where surface melt is greater.

459 ~~Figure 7 shows a~~ The schematic ~~of~~in Figure 7 depicts how ~~the~~glacier elevation and hypsometry ~~of glaciers is~~are

460 likely to influence the distribution and density of supraglacial channels in alpine settings. The lowest drainage

461 densities are predicted to occur on smaller cirque glaciers due to their lower meltwater supply, restricted distance

462 for meltwater to coalesce into channels, and increased channel ~~inception~~interception due to crevasses on often

463 steeper slopes (Fig. 7A). Whilst we detect very few channels ~~>0.5 m~~ on cirques due to our imagery resolution,

464 these glaciers likely still contain networks of smaller channels ~~networks~~. By comparison, larger valley glaciers

465 (e.g., Grosser Aletschgletscher) tend to exhibit moderate to high drainage densities because they produce high

466 amounts of meltwater, but much of it may be intercepted by crevasses on steeper slopes, preventing or restricting

467 large channel formation (Fig. 7B). The glaciers with the highest drainage densities are likely to have a large

468 ~~ablation~~snow-free area (high meltwater supply) and occur on lower slopes because fewer crevasses allow large

469 drainage networks to become established (Fig. 6; Fig. 7C). One example of this configuration is the Oberer

470 Theodulgletscher which ~~contains~~has the ~~largest~~highest drainage density ~~in our study area~~among Valais glaciers

471 (Fig. 4a). It is possible that its high drainage density is also due to its location on a ~~slightly higher~~high elevation

472 plateau, because air temperatures are likely to be cooler than at the ~~terminus~~termini of neighbouring glaciers which

473 extend further down valley (Fig. 5f). As a result, the rate of surface lowering is likely ~~lower~~slower, meaning that

474 lower rates of incision are needed for channel formation to keep pace with surface lowering, resulting in a higher

475 drainage density (~~Rippin et al., 2015;~~Pitcher ~~&~~and Smith, 2019). However, summer temperatures in the Alps are

476 increasing (Sommer et al., 2020), which will result in higher rates of surface lowering, meaning that all glaciers,

477 but more specifically those with larger portions of their ~~mass~~area at lower elevations, will require increased

478 channel incision to counteract the higher rates of surface lowering ~~in order for channels to form. Higher rates of~~

479 ~~surface melt may, however, counteract this process by increasing the potential for channel incision.~~(Marston,

480 1983).
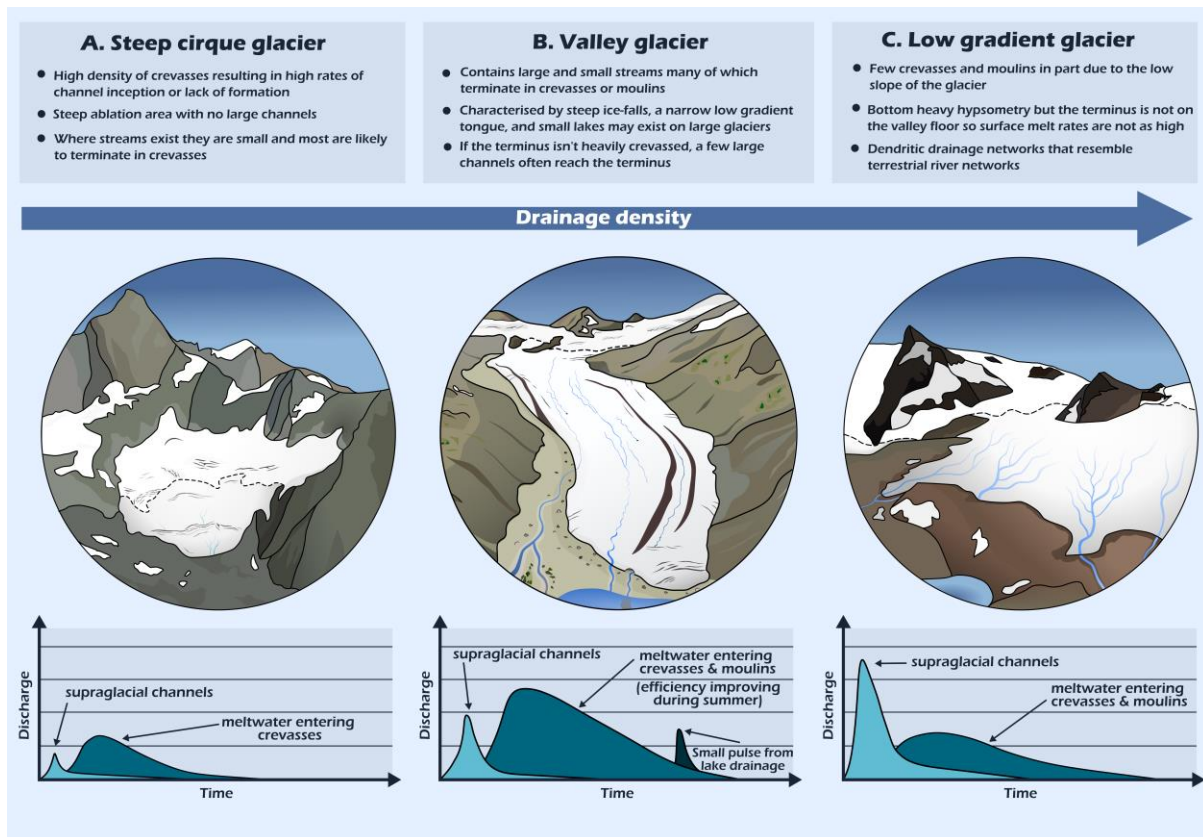
Figure 7: A schematic depicting the range of glacier types (A-C) and their respective characteristics, increasing in drainage density from left to right. Each glacier type corresponds to a hypothesised hydrograph (bottom) depicting changes in proglacial channel discharge over an unknown time period (ranging from minutes to days) as a response to a surface melt event. The hydrographs are hypothesised to represent the general characteristics of each glacier's runoff regime (see text for discussion) and do not reflect the complexities of individual measured proglacial stream discharge. Light blue shading shows the hypothesised hydrograph if all ~~of~~ the meltwater were to be transported via supraglacial channels, whereas those shown in ~~mid~~ medium blue show the hydrograph where the bulk of meltwater is transported englacially/subglacially. Dark blue in panel (b) shows a lake drainage event.

The distribution and density of channels on different types of glaciers ~~is also~~will likely ~~to~~ impact the runoff hydrograph (Fig. 7). ~~Small~~At small cirque glaciers ~~(Fig. 7A) are typically characterised by steep, heavily crevassed slopes, meaning meltwater is more likely to be captured by crevasses, and there is limited distance for meltwater to coalesce and form channels. Hence,~~ runoff ~~at cirque glaciers~~ in response to surface melt is likely characterised by a small earlier peak from a few supraglacial channels (light blue shading in Fig. 7A) or a slightly delayed peak as crevasses capture meltwater and route it through the en- (and -sub) glacial ~~system (dark~~drainage systems (medium blue shading in Fig. 7A~~).)~~ (e.g., Clason et al., 2015). By comparison, valley glaciers are ~~frequently characterised by~~ larger ~~non-crevassed zones, meaning~~and tend to contain more ~~meltwater reaches the terminus supraglacially~~supraglacial channels, but channels are often intercepted by crevassed zones or ice falls. This may result in an initial peak in meltwater from supraglacial channels, followed by a delay in meltwater routed

502 en- (and sub-) glacially (Fig. 7B~~), with a progressively reduced~~). Over the melt season, the lag time between melt

503 and peak proglacial discharge ~~throughout the melt season~~typically decreases due to increased subglacial drainage

504 network efficiency (Nienow et al., 1998). Additionally, some larger valley glaciers contain small supraglacial and

505 ice marginal lakes (e.g., Gornergletscher and Grosser Aletschgletscher), which may experience infrequent

506 drainage events (e.g., Huss et al., 2007), leading to a sudden peak in proglacial river discharge. Whilst less

507 common in Valais, glaciers characterised by large~~, low angle ablation~~ shallow sloping areas often contain

508 ~~large~~extensive supraglacial drainage networks that capture the majority of surface melt (Fig. 7C).~~.~~ This is because

509 ~~low angle ablation areas~~shallow slopes typically have smaller and fewer crevasses than most valley glaciers ~~(Fig.~~

510 ~~7C).~~ They will tend to have the 'flashiest' hydrograph because the supraglacial drainage network rapidly transfers

511 melt off the glacier surface. ~~Where a small number~~Interception of this drainage by crevasses or moulins ~~intercept~~

512 ~~this drainage, it leads to a more lagged~~will increase the lag and decrease the amplitude of the hydrograph response

513 ~~and with a peak well below the hydrograph from supraglacial channel drainage.~~.

514 Our dataset provides new insight into supraglacial channel distribution across a large range of glaciers, allowing

515 simple inferences to be made about connectivity and possible lag times between melt and peak proglacial

516 discharge based on the locations of our mapped channel termini. Overall, we find that ~~72% of our mapped highest~~

517 ~~order channel segments route meltwater to en- or subglacial positions and 25% run off~~ at the average Valais glacier

518 ~~margin, 80% of channels run directly off the glacier, while the remaining 20% terminate in moulins or crevasses~~.

519 However, this varies between glaciers and in the case of the largest glacier, Grosser Aletschgletscher~~,~~ (type B in

520 Fig. 7), no mapped channels reach the terminus~~; attributed to the location~~ because of highly crevassed zones

521 forcing meltwater into the glacier (53 % of channels enter moulins and 36 % enter crevasses). Unlike most glaciers

522 in the Alps, small supraglacial lakes are also present on the Grosser Aletschgletscher, which capture 11 % of its

523 channels. By comparison, the Oberer Theodulgletscher~~,~~ (type C in Fig. 7), which exhibits the highest drainage

524 density ~~within our dataset~~, contains almost no moulins (2.8 % of channel termination~~)~~). and 27 % of channels

525 reach the terminus or periphery. A large number of channels terminate in crevasses on the Oberer Theodulgletscher

526 (70 %), but crevasses tend to be small (< 0.3 m wide~~)~~). and it is not known whether meltwater enters englacially

527 or is routed ~~supraglacially~~on the glacier surface through trace crevasses (e.g., Fig. 8). Observations have shown

528 that trace crevasses may act as a preferential meltwater pathway, often resulting in channels forming perpendicular

529 to ice flow (e.g., Chen et al., 2024). However, crevasses may also fill with meltwater and be continually overtopped

530 if a channel is situated in a compressive regime, and thus less prone to hydrofracture (e.g., Chudley et al., 2021).

531 As the true location of channel termination is unknown, our channel segments are always broken at crevasses if a

532 clear pathway cannot be identified.

533

534
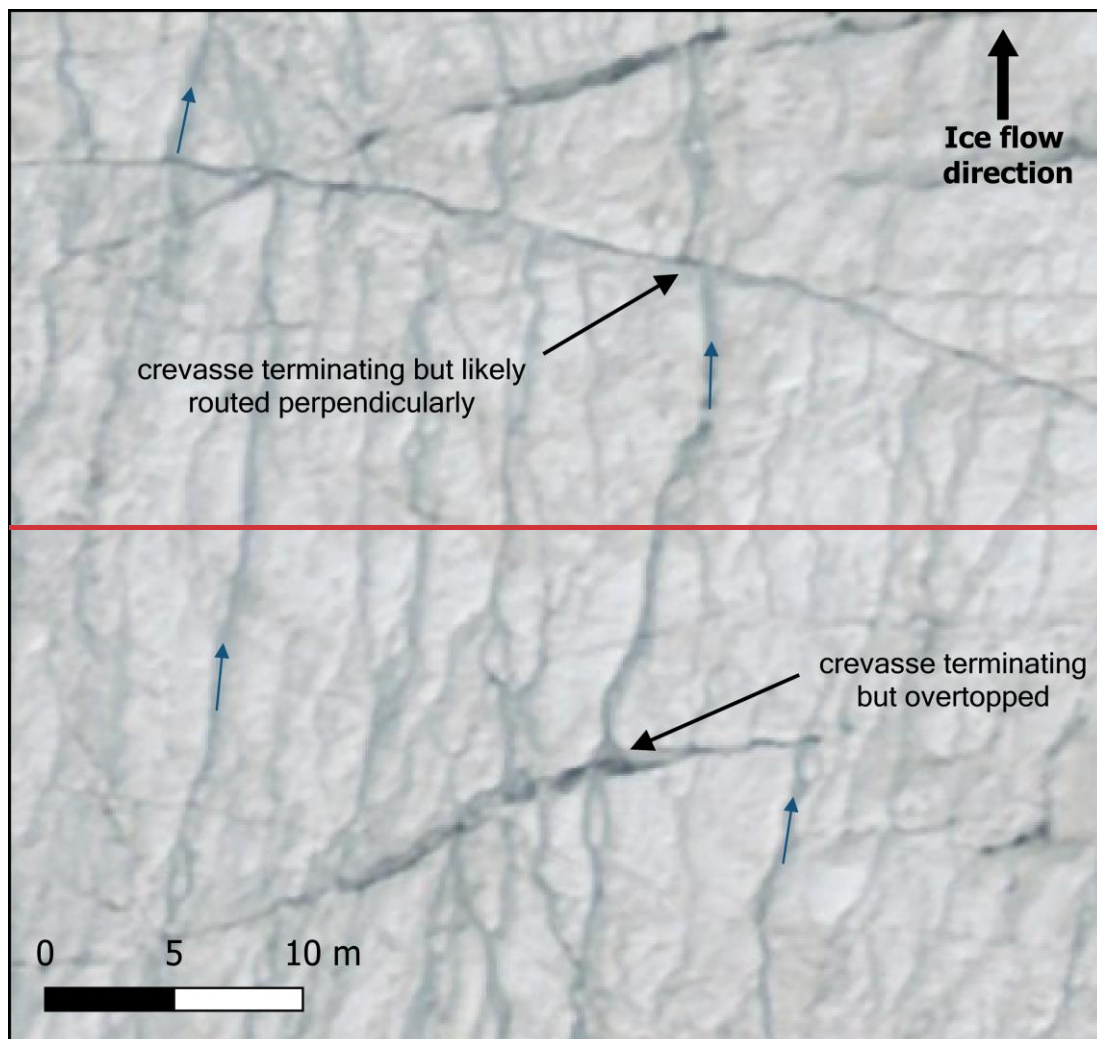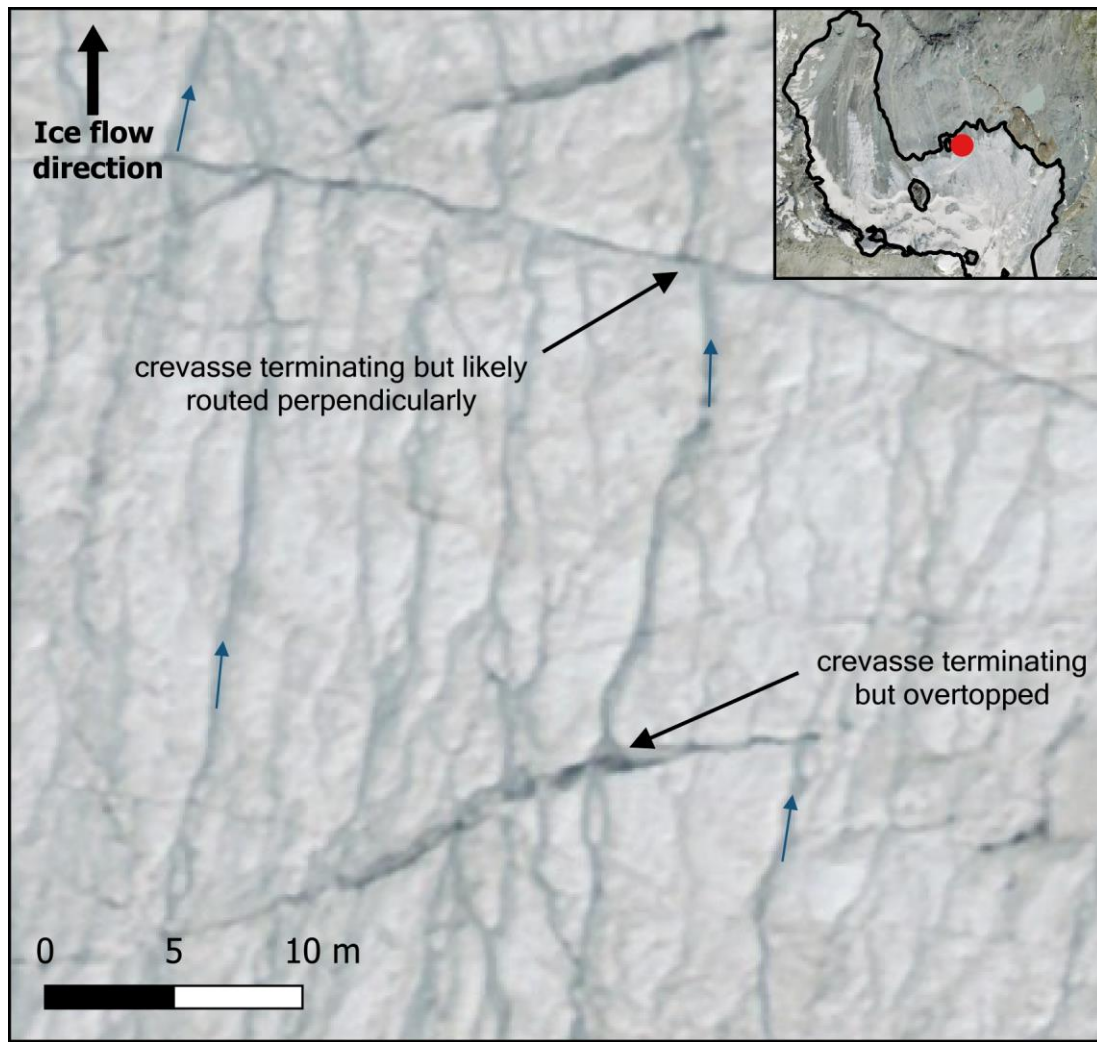
Figure 8: Examples of channels terminating in crevasses on the Oberer Theodulgletscher. The location of the main panel is shown in red on the glacier (top right). Channels are shown to terminate in crevasses but often continue directly down-glacier as some meltwater overtops the crevasse. Small blue arrows indicate the direction of meltwater flow, with meltwater broadly flowing from the bottom to the top of the image. Imagery source: Federal Office of Topography ~~swisstopo~~Swisstopo.

The difference in drainage pathways between the Oberer Theodulgletscher ~~compared to~~and the Grosser Aletschgletscher can be explained by the difference in glacier type outlined in Figure 7~~, which classifies glaciers based upon their slope and hypsometry.~~. At the Grosser Aletschgletscher, increased meltwater capture by crevasses and moulins likely ~~allows for~~facilitates increased surface-to-bed meltwater transfer, which is supported by observations of its ~~seasonal~~summer speed-up in ice flow velocity (Leinss and Bernhard, 2021). Model simulations suggest that increased meltwater presence at the glacier bed increases the excavation of subglacial sediment (Delaney and Adhikari, 2020), which would result in higher proglacial stream sediment concentrations~~,~~ if streams are not diluted by freshwater flux from proglacially terminating supraglacial channels. This is important for regions such as the Alps because proglacial stream sediment concentrations can directly impact agriculture and

550 hydropower infrastructure (Micheletti and Lane, 2016). Hence, categorising glaciers based on their slope and

551 hypsometry is beneficial because it provides insight into the anticipated drainage density of a glacier, ~~the~~

552 ~~likely~~probable channel pathways (i.e., sub-/englacially or ~~supraglacially~~proglacially terminating), and whether a

553 higher amount of surface-to-bed meltwater transfer is ~~to be predicted~~likely.

554

~~5.2~~ Controls on channel ~~morphology~~

556 ~~5.2~~   ~~In Valais Canton, channel~~ **morphometry** ~~varies significantly between channels, with highly sinuous~~
557   ~~channels (e.g., Fig. 4d-e) observed to occur on some glaciers but not others. We find that slope~~
558   ~~affects sinuosity (Fig. 5a); the most sinuous channels are likely to occur on lower angle slopes (0 to~~
559   ~~10°) and channels on steeper slopes (> 20°) are unlikely to exhibit a sinuosity over 1.3. Our~~
560   ~~observations find that wider and more incised channels (which are likely to have higher discharge)~~
561   ~~tend to be more sinuous (e.g., Fig. 4d-e). The importance of discharge as a control on sinuosity is~~
562   ~~supported by St Germain & Moorman (2019) who attribute higher channel sinuosity to increased~~
563   ~~channel discharge on glaciers in the High Arctic. They also find that channels on higher angle~~
564   ~~slopes tend to be more sinuous, which is not observed for channels in Valais (Fig 5a). Similarly,~~
565   ~~higher slopes have been found to increase supraglacial channel incision (Gulley et al., 2009), which~~
566   ~~based on our observations of high sinuosity channels being deeply incised in Valais suggests that~~
567   ~~incision (from either slope and/or channel discharge) is needed for the production of highly sinuous~~
568   ~~channels. These channels are likely to continue to evolve inter-annually due to their incised depth.~~
569   ~~Given this, we suggest that the relationship between slope and sinuosity in~~ ~~Fig. 5a~~ ~~represents the~~
570   ~~conditions under which large channels can form (i.e., flatter, less crevassed regions) rather than the~~
571   ~~direct impact that slope has on sinuosity. This differs to the High Arctic glaciers observed by St~~
572   ~~Germain & Moorman (2019) where slope is a clear control on channel sinuosity. We attribute this~~
573   ~~difference to the cold-based High Arctic glaciers typically being less crevassed, resulting in a larger~~
574   ~~viable area for channel formation (i.e., not solely restricted to smaller, flat, less crevassed zones),~~
575   ~~and because incision to a deeper depth is likely aided by lower rates of surface lowering.~~

576 In Valais, there is a large variation in sinuosity values, with sinuous channels (1.05 - 1.25) occurring on some

577 glaciers but not others. We find that slope affects sinuosity, with the most sinuous channels (2.5 - 1.5) likely to

578 occur on lower angle slopes (0 to 10°) (Fig. 5a); in contrast, channels on steeper slopes (> 20°) typically do not

579 exhibit a sinuosity over 1.3. Channels tend to be least sinuous on debris-free ice, slightly more sinuous on thicker

580 debris cover, and the most sinuous on moderately debris-covered ice (Fig. 5c). However, the most sinuous

581 channels are found on predominantly debris-free ice on Gornergletscher (Fig. 4e). The high prevalence of sinuous

582 channels on moderately debris-covered ice may be due to increased sediment in the channels, sourced from the

583 surrounding terrain, which was also found to increase channel sinuosity at an Alaskan glacier (Boyd et al., 2004).

584 However, the relationship we observe between slope and sinuosity in Valais (Fig. 5a) differs from the findings of

585 St Germain and Moorman (2019), who found that channels on a High Arctic glacier were more sinuous on steeper

586 slopes. This difference may be explained by three factors. The first is that channel distribution in Valais is heavily

587 influenced by crevassed areas (Fig. 5b; Fig. 6), meaning that channel formation is more likely on flatter areas with

588 fewer crevasses. A second consideration is channel discharge, which we do not measure here. Discharge and slope

589 control stream power, which has been found to positively correlate with sinuosity (Ferguson et al., 1973; Marston,

590 1983; St Germain and Moorman, 2019). We cannot separate out the relative impacts of slope and discharge.

591 However, higher discharges are most likely to form on flatter areas with fewer crevasses, as they favour the

592 development of longer channels (e.g., Fig.

~~Our mapping also reveals some distinct differences in appearance and sinuosity between clean and debris covered glaciers in Valais. Channels that have a proximal debris source and those that run directly through debris cover tend to be more sinuous than channels on clean ice (Fig. 5c), with a statistically significant difference between the classes (p = <0.05 in an ANOVA test). Figure 4d shows large meandering channels on a debris covered glacier (Oberaletschgletscher), with channels on clean glaciers not being as sinuous. On debris covered glaciers, we commonly observe less sinuous channels at higher elevations with less debris cover. These less sinuous channels are then funnelled through areas of bare exposed ice until reaching continuous debris cover where large meandering planforms begin to develop. These channels are anticipated to transport the majority of glacier surface melt as there is a general absence of visible small channels on debris covered glaciers in Valais, and meltwater transport within the debris matrix is slow and dispersed (Fyffe et al., 2019). Due to high channel incision, some of these debris covered glaciers (e.g.,~~ 5b). Additionally, reduced meltwater interception in flatter areas allows more meltwater to enter channels, potentially increasing sinuosity. Finally, the sediment cover of many glaciers in Valais exceeds that of the glacier examined by St Germain and Moorman (2019). Hence, channel sediment content is likely higher in Valais, which may increase channel sinuosity due to enhanced erosion during sediment transport or, alternatively, reduce erosion where the bed is covered by thick sediment. Overall, the difference in relationship between slope and sinuosity between Valais and a glacier High Arctic is attributed to the effect of multiple independent variables on sinuosity, which differ in impact between locations.

~~Fig. 4d) have exposed channel banks of bare ice which are too steep to support debris cover. The exposure of non-insulated ice by channel incision likely exacerbates meltwater production and channel discharge, furthering channel development (e.g., Mölg et al., 2019). Additionally, the increased sediment presence within channels, which would be expected on highly debris covered glaciers, may also support channel development. Whilst previous research has documented channels on debris covered glaciers in mountain glacier regions (e.g., Benn et al., 2017), there has been limited assessment of the effect of debris within supraglacial channels on channel morphometry. This remains poorly understood as most supraglacial research has occurred on ice sheets, where areas of lower albedo are controlled by the presence of, dust, black carbon, algae, and cryoconite deposits (e.g., Ryan et al., 2018; Leidman et al., 2021; Khan et al., 2023).~~

~~Further insight may be gained from bedrock rivers, which contain a mixture of sediment cover and exposed bedrock. In bedrock rivers, sediment was found to increase channel erosion rates and increase sinuosity, but high sediment supply may reduce erosion due to producing sediment cover which protects the bed from erosion (Moore, 1926; Shepherd, 1972; Turowski, 2018). Ultimately, future work is needed to determine the role of debris in supraglacial systems, specifically in situ measurements of debris content in channels to determine how it affects channel properties.~~

5.3   Comparison between ~~mountain~~Valais glaciers and ~~ice sheets~~ the Greenland Ice Sheet

Previous research on supraglacial channel morphometry has predominantly focused on ~~ice sheet settings~~the GrIS (e.g., Smith et al., 2015; Karlstrom ~~&~~and Yang, 2016; Yang ~~&~~and Smith, 2016; Yang et al., 2016, 2021, 2022),

630 ~~hence it is important to establish how comparable channels on ice sheets are to those on mountain glaciers.~~

631 ~~Similarities~~with some similarities in drainage patterns ~~are~~ observed between the ~~two environments, for~~GrIS and

632 Valais glaciers. For example, in Valais, larger glaciers often contain dendritic drainage patterns (e.g., 4a), which

633 ~~is~~are commonly observed ~~in an ice sheet setting~~on the GrIS (e.g., Yang et al., 2016, 2019). However, ~~in Valais~~

634 some glaciers ~~contain~~in Valais display parallel, ~~less~~weakly interconnected channel networks ~~because there is~~,

635 likely ~~not sufficient~~due to insufficient distance for meltwater to ~~coalesce.~~converge into a single channel. It

636 ~~would~~could be expected that, given sufficient distance for meltwater to coalesce, these networks would be

637 comparable to networks on ~~ice sheets~~the GrIS, which broadly follow Horton's laws, i.e., mean river length

638 increases with channel order and mean slope decreases with channel order (Yang et al., 2016). On a smaller scale,

639 ice surface structures (e.g., trace crevasses ~~and flow stripes) have been found to~~) exhibit a strong control on

640 meltwater routing ~~in both~~on Valais glaciers ~~in Valais~~ and on both the Greenland and ~~on~~Antarctic ice sheets~~,~~

641 ~~meaning that channels do not always follow the steepest path over the ice surface~~ (e.g., ~~Figs. 5c & 9~~Fig. 4c; Chen

642 et al., 2024).

643 ~~Some differences exist between ice sheets and glaciers in~~ Nevertheless, Valais~~, such as debris may play a larger~~

644 ~~role in channel formation in mountain environments. For example,~~ and the GrIS differ in where channels ~~have~~

645 ~~been observed to form parallel to medial moraines due to topographic confinement~~terminate, and ~~debris creates~~

646 ~~an uneven albedo and higher surface roughness which may increase channel~~ their glacier surface characteristics

647 are often dissimilar (e.g., debris coverage). On the southwest~~density (Rippin et al., 2015). Glaciers in Valais also~~

648 ~~exhibit notable differences in coupling between surface melt and the englacial/subglacial system compared to the~~

649 ~~SW GrIS. On the SW~~ GrIS, virtually all higher-order channels ~~are observed to~~ terminate in moulins (Smith et al.,

650 2015), whereas ~~in~~at the average Valais ~~72~~glacier, only 20 % of ~~highest order~~our mapped channels terminate

651 englacially ~~(37% in crevasses and 35% in moulins). Additionally, there is~~. This suggests notable differences in

652 coupling between surface channels and the englacial/subglacial system. There is also a general absence of

653 supraglacial lakes in Valais, except for small lakes on Gornergletscher and the Grosser Aletschgletscher, meaning

654 few channels terminate in lakes, whereas ~~they~~lakes exist in abundance on the GrIS (Chu, 2014). ~~On the GrIS,~~

655 ~~supraglacial lakes act as temporary storage, with the potential for meltwater to refreeze rather than reaching the~~

656 ~~terminus each melt season; however, hydro-fracture events can cause rapid lake drainage, which has been linked~~

657 ~~to ice speed up events (e.g., Das et al., 2008; Morriss et al., 2013; Chudley et al., 2019). In mountain glacier~~

658 ~~environments, the general higher surface slopes and absence of temporary supraglacial storage means that~~

659 ~~proglacial discharge~~Additionally, debris cover is more extensive in Valais and is observed to affect channel

660 morphology (see section 5.2) and distribution. The latter is evident from the formation of channels parallel to

661 lateral or medial moraines due to topographic confinement (e.g., Fig. ~~clearly linked to rates of surface melt, with~~

662 ~~few sudden pulses of~~4b). Debris cover also modulates surface melt and influences both micro-scale and larger-

663 scale surface roughness, which in some cases has been associated with increased channel density (Rippin et al.,

664 2015). However, whilst the scale of sediment coverage differs, the presence of dust, black carbon, algae, and

665 cryoconite deposits on the GrIS may still affect channel distribution and morphometry (e.g., Ryan et al., 2018;

666 Leidman et al., 2021; Khan et al., 2023).~~discharge except for in regions prone to glacial lake outburst floods (e.g.,~~

667 ~~High Mountain Asia).~~

668

5.4   Future evolution of supraglacial channel systems

The ~~role~~impact of climatic warming on supraglacial drainage networks is ~~unclear~~not fully understood, but we suggest that supraglacial drainage networks ~~will develop and~~may expand to higher elevations due to rising equilibrium lines (Leeson et al., 2015). Whether discharge in current channels will increase or decrease ~~is dependent~~depends on the ~~rate~~rates of glacier retreat and ~~summer melt~~surface lowering, driven by ablation. It is likely that larger glaciers will see an increase in channel discharge due to rising equilibrium lines and ~~subsequent~~associated higher rates of surface melt (St Germain ~~&~~and Moorman, 2019). However, the reduction in area for smaller glaciers may be large enough to prevent the formation of ~~established~~efficient drainage networks~~, and changes~~. Changes in glacier slope ~~may~~could also result in a reconfiguration of the drainage system (e.g., new crevasses may intercept channels that formerly reached the terminus~~) or a reduction in~~), which may affect drainage density (Fig. 5e). Additionally, glaciers in some mountain ~~glacier~~ environments are undergoing an increase in debris cover (e.g., Glasser et al., 2016; Fleischer et al., 2021), and it is not fully understood how changes in debris cover will affect surface meltwater supply and transport, channel morphometry and morphology~~,~~. and surface albedo (e.g., Leidman et al., 2021). Future research ~~would~~could benefit from utilising the growing repository of high-resolution orthophoto surveys to ~~inform~~improve our understanding of supraglacial hydrology ~~outside of ice sheet~~ in mountain glacier settings~~, particularly concerning~~. Increased understanding of seasonal and interannual channel evolution is needed to better inform modelling of glacier hydrology. ~~It~~For example, it is not ~~currently known how widely applicable~~clear whether our ~~research is~~findings would also apply to regions with larger glaciers and lower rates of surface lowering (e.g., the Arctic~~)~~), so future studies ~~may benefit from assessing their similarity~~could repeat our work in such regions. Lastly, further in-situ measurements would be beneficial to determine whether the channels delineated as part of this study represent the majority of meltwater transport on ~~mountain~~Valais glaciers~~,~~ or whether channels below our mapping resolution also play a key role in meltwater transport.

6   Conclusion

This study presents the first comprehensive dataset on the distribution and characteristics of supraglacial channels at a regional scale in a mountain glacier environment. ~~We mapped 1890 channel segments >0.5 m wide on~~Out of 285 glaciers in Valais Canton, Switzerland, we identified 85 glaciers ~~found to contain~~that contained channels above our mapping resolution ~~in Valais Canton, Switzerland, out of a total sample of 285 glaciers. We found large~~(0.5 m wide). We found substantial variability in ~~channel~~glacier drainage ~~densities between glaciers~~density, with the highest ~~drainage densities~~values occurring on glaciers ~~characterised by low~~with shallow slopes~~, with~~ and a large portion of their surface area at lower elevations (Fig. 7). The presence of channels is primarily dictated by a sufficiently ~~large~~supply of meltwater (i.e., large enough glacier area) and an uninterrupted distance for meltwater to coalesce (i.e., absence of crevasses~~and low ice surface slopes~~). The primary control on channel distribution is surface topography, with the slope and size of the ~~ablation~~snow-free area providing a clear limit on both where channels can form and their total length (Fig. 5b). However, strong structural controls on channel distribution exist~~, for~~. For example, trace crevasses have been observed to act as preferential meltwater pathways, resulting in channels forming perpendicular to ice flow. Channels also commonly form parallel to medial and lateral moraines

due to topographic confinement. Most channels are characterised by low sinuosity (Fig. 5a), ~~with a general absence of the canyon-like channels described on cold or polythermal glaciers. However,~~although some highly sinuous channels ~~exist~~are present, particularly on moderately debris-covered ~~glaciers characterised by channels with steep~~ice ~~cliffs~~and ~~on low slope~~lower-relief glacier termini~~, with~~. This contrasts with cold or polythermal glaciers, where sinuous channels ~~most~~are more commonly ~~occurring where channels are also deeply incised~~found on steeper slopes. These findings suggest that controls on channel morphology and morphometry are not consistent across mountain glacier environments and may instead reflect variations in debris cover, the location and density of crevassed zones, and rates of surface lowering.

~~Glaciers in~~In Valais~~,~~, most glaciers are characterised by a ~~large~~high proportion of channels ~~reaching~~that reach the glacier margin ~~rather than terminating englacially. When~~without being routed into the ~~channel termini locations are calculated~~glacier. On average, approximately 80 % of channels ~~per glacier, the average glacier would have 80% of its channels~~ run directly off the glacier ~~while 20% would~~ (terminate ~~englacially. Overall,~~proglacially), while the remaining 20 % terminate in a crevasse or moulin. We find that 48 % of glaciers ~~contain no englacially~~support only proglacially terminating channels, ~~compared to only~~whereas 3.5 % of glaciers ~~where all channels terminate~~are characterised by entirely englacially-terminating channels. The location of channel termini (i.e., ~~supraglacial~~proglacial or englacial) is hypothesized to produce different hydrograph responses to surface melt, some of which we suggest may be more common for certain glacier hypsometries~~. The observed channel~~ (Fig. 7). Channel terminus locations in Valais ~~differs~~differ from ~~typical ice sheet settings where very few supraglacial~~those described in prior research, which has largely focused on the SW GrIS, where most channels terminate in moulins and very few reach the ice margin~~, with most surface melt transported englacially through crevasses or moulins. In comparison to ice sheets, channel~~. Similar to the GrIS, drainage networks ~~in mountain glacier environments~~on Valais glaciers often exhibit dendritic patterns. However, such configurations are ~~often~~likely less ~~established~~widespread due to ~~glaciers having~~smaller drainage areas and ~~there being less~~limited distance for channels to ~~coalesce, with valley glaciers often narrowing down-glacier reducing the possible size of drainage networks.~~merge.

~~7   Supplementary Data~~

Appendix A: Principal Component Analysis

742 **Table S1A1: The eigenvectors for principal components 1 to 6 from a PCA analysis of glacier and channel**
743 **characteristics, with PC1 being the most significant. The three largest loadings for each principal**
744 **component are in bold.**

745

	PC1	PC2	PC3	PC4	PC5	PC6
Glacier area	**-0.439**	0.042	0.034	0.288	-0.187	0.054
Glacier minimum elevation	**0.435**	-0.112	0.085	-0.098	**0.407**	-0.178
Channel maximum elevation	**0.393**	0.159	0.066	**0.436**	-0.115	0.186
Channel length	-0.070	-0.264	**-0.582**	0.312	0.195	**-0.199**
Channel minimum elevation	0.382	0.196	0.121	**0.423**	-0.100	0.196
Channel sinuosity	-0.117	-0.182	-0.122	-0.041	**0.468**	**0.845**
Channel elevation range	0.166	-0.345	**-0.542**	0.198	-0.173	-0.068
Channel slope	0.320	-0.203	-0.066	-0.115	**-0.483**	**0.255**
Drainage density	0.131	**0.543**	-0.268	-0.009	0.041	0.083
Mean glacier slope	0.119	**-0.439**	0.136	-0.309	-0.335	0.141
Glacier mean elevation	0.170	**-0.376**	**0.401**	0.280	0.339	-0.188
Glacier max elevation	-0.330	-0.175	0.264	**0.462**	-0.163	0.086

746
747
748
749
750
751

752
753
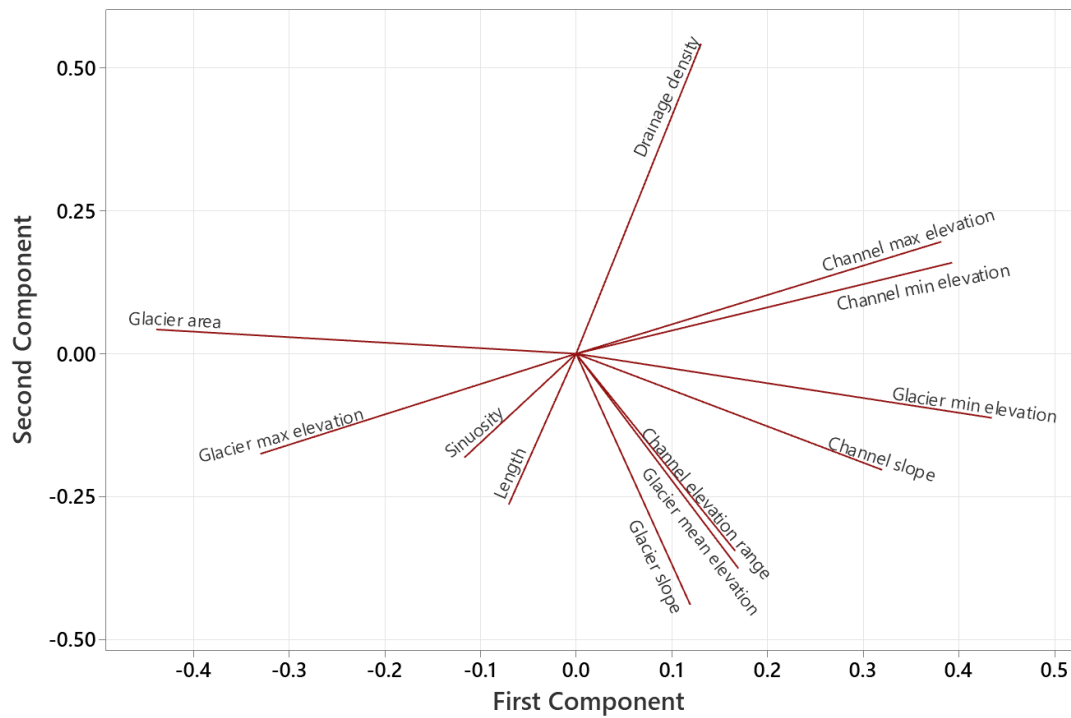
754 **Figure ~~S1: loading~~A1: Loading plot for principal components 1 and 2 from a PCA analysis of glacier and**
755 **channel characteristics.**
756
757
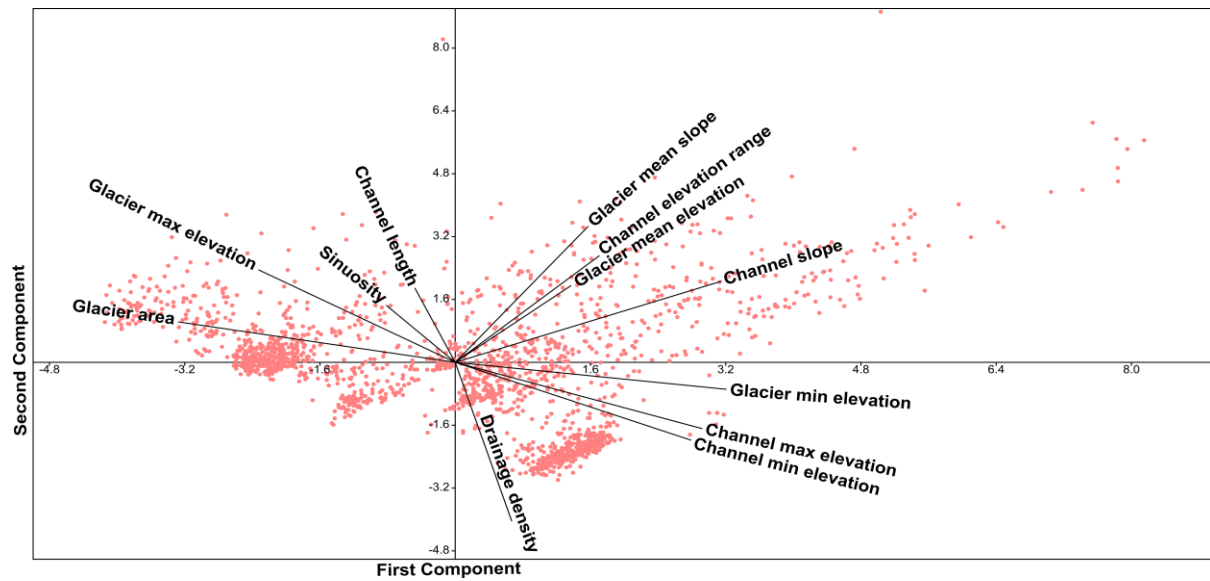
758
759
760 **Figure ~~S2~~A2: A biplot from a PCA analysis showing principal components 1 and 2, which ~~was~~were used for**
761 **~~cluster analysis~~visually identifying clusters and overlayed with a loading plot (see Fig. ~~S1~~A1).**

762

763

764

765 **Appendix B: Accuracy Assessment**

766
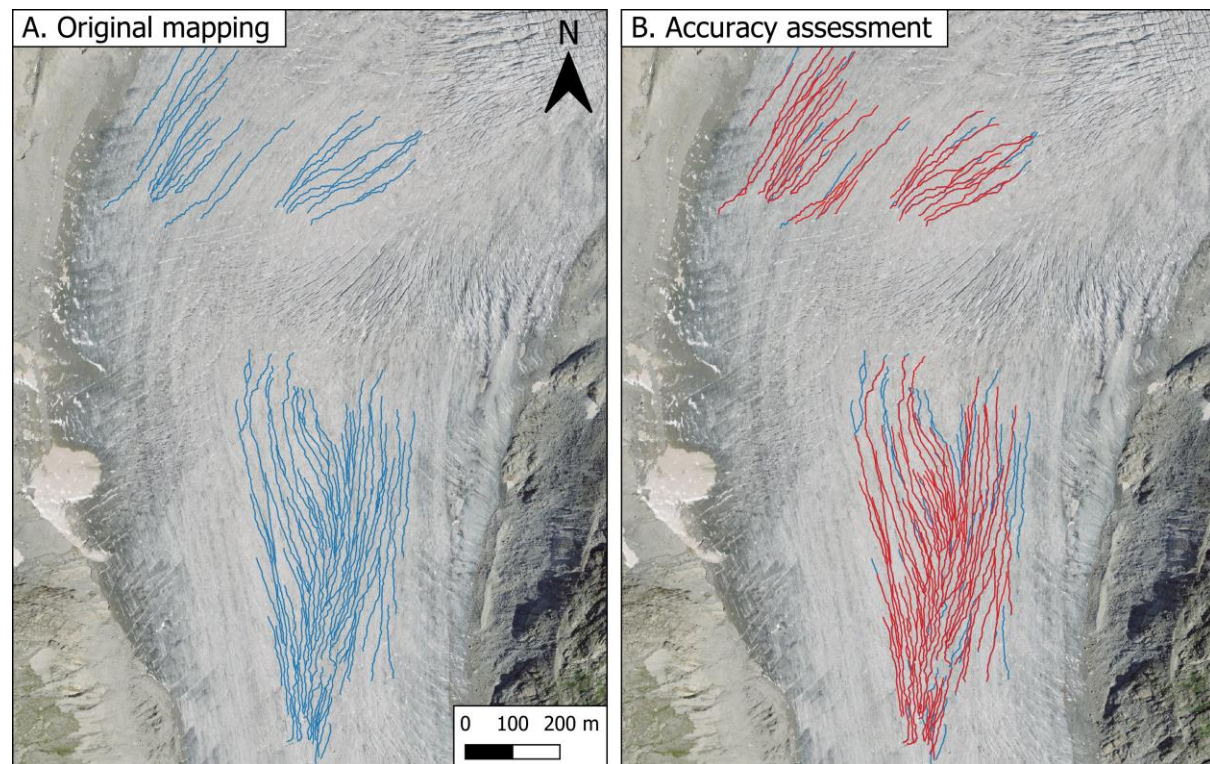
Figure ~~S3~~B1: Repeat mapping of the Rhonegletscher used to determine mapping accuracy. (A) Mapping from this dataset is shown in blue. (B) A comparison between the repeat mapping (red) and the original mapping (blue~~), which)~~ was undertaken independently after several weeks had elapsed.

Data availability

The orthophoto and DEM data used in this study are freely available on the SwissTopo website (https://www.swisstopo.admin.ch/). Outlines of glaciers in Valais were obtained from Glacier Monitoring in Switzerland (GLAMOS) and are available online (https://glamos.ch/). The produced supraglacial channel data is available upon request from the corresponding author (Holly Wytiahlowsky: holly.e.wytiahlowsky@durham.ac.uk).

Author contributions

All authors contributed to the conceptualisation of this project. HW conducted the mapping, ~~formal~~ analysis and data visualisation under the supervision of CRS, RAH, CCC and SSRJ. HW led manuscript writing with comments and ~~revisions~~edits provided by all authors.

Competing interests

CC is a member of the editorial board of The Cryosphere, and CRS was a member at the time of submission.

Acknowledgements

This work was supported by the Natural Environment Research Council via an IAPETUS2 PhD studentship held by Holly Wytiahlowsky (grant reference NE/S007431/1). We thank SwissTopo for making their orthophotos and DEM data open access. We thank two anonymous reviewers and Ian Willis for their constructive feedback, which has helped to improve this paper, and Kang Yang for acting as editor for the manuscript.

~~8~~7 References

Bamber, J. L., Oppenheimer, M., Kopp, R. E., Aspinall, W. P., and Cooke, R. M.: Ice sheet contributions to future sea-level rise from structured expert judgment, Proc. Natl. Acad. Sci., 116, 11195–11200, doi:10.1073/pnas.1817205116, 2019.

Banwell, A., Hewitt, I., Willis, I., and Arnold, N.: Moulin density controls drainage development beneath the Greenland ice sheet, J. Geophys. Res. Earth Surf., 121, 2248–2269, doi:10.1002/2015JF003801, 2016.

800 Bell, R. E., Chu, W., Kingslake, J., Das, I., Tedesco, M., Tinto, K. J., Zappa, C. J., Frezzotti, M., Boghosian, A.,
801 and Lee, W. S.: Antarctic ice shelf potentially stabilized by export of meltwater in surface river, Nature, 544,
802 344–348, doi:10.1038/nature22048, 2017.

803 Benn, D. I., Thompson, S., Gulley, J., Mertes, J., Luckman, A., and Nicholson, L.: Structure and evolution of the
804 drainage system of a Himalayan debris-covered glacier, and its relationship with patterns of mass loss,
805 Cryosphere, 11, 2247–2264, doi:10.5194/tc-11-2247-2017, 2017.

806 Brice, J. and Blodget, J.: Countermeasures for Hydraulic Problems at Bridges, Volume 1 – Analysis and
807 Assessment.

808 Boyd, B., Goetz, S. L., and Ham, N. R.: Supraglacial stream incision into debris-covered ice, Matanuska
809 Glacier, AK. Geol. Soc. Am. Abstr., 36, 11.

810 Carey, M., Molden, O. C., Rasmussen, M. B., Jackson, M., Nolin, A. W., and Mark, B. G.: Impacts of glacier
811 recession and declining meltwater on mountain societies, Ann. Am. Assoc. Geogr., 107, 350–359,
812 doi:10.1080/24694452.2016.1243039, 2017.

813 Chen, J., Hodge, R. A., Jamieson, S. S. R., and Stokes, C. R.: Distribution and morphometry of supraglacial
814 channel networks on Antarctic ice shelves. J. Glaciol., doi:10.1017/jog.2024.99, 2024.

815 Chu, V. W.: Greenland Ice Sheet hydrology: A review, Prog. Phys. Geogr., 38, 19–54,
816 doi:10.1177/0309133313507075, 2014.

817 Chudley, T. R., Christoffersen, P., Doyle, S. H., Bougamont, M., Schoonman, C. M., Hubbard, B., and James,
818 M. R.: Supraglacial lake drainage at a fast-flowing Greenlandic outlet glacier, Proc. Natl. Acad. Sci., 116,
819 25468–25477, doi:10.1073/pnas.1913685116, 2019.

820 Chudley, T. R., Christoffersen, P., Doyle, S. H., Dowling, T. P. F., Law, R., Schoonman, C. M., Bougamont, M.,
821 and Hubbard, B.: Controls on Water Storage and Drainage in Crevasses on the Greenland Ice Sheet, J. Geophys.
822 Res. Earth Surf., 126, e2021JF006287, doi:10.1029/2021JF006287, 2021.

823 Clason, C. C, Coch, C., Jarsjö, J., Brugger, K., Jansson, P., and Rosqvist, G.: Dye tracing to determine flow
824 properties of hydrocarbon-polluted Rabots glaciär, Kebnekaise, Sweden, Hydrol. Earth Syst. Sci., 19, 2701–
825 2715, doi:10.5194/hess-19-2701-2015, 2015.

826 Clason, C. C, Rangecroft, S., Owens, P. N., Łokas, E., Baccolo, G., Selmes, N., Beard, D., Kitch, J., Dextre, R.
827 M., Morera, S., and Blake, W.: Contribution of glaciers to water, energy and food security in mountain regions:
828 current perspectives and future priorities, Ann. Glaciol., 63, 73–78, doi:10.1017/aog.2023.14, 2023.

829 Das, S. B., Joughin, I., Behn, M. D., Howat, I. M., King, M. A., Lizarralde, D., and Bhatia, M. P.: Fracture
830 propagation to the base of the Greenland Ice Sheet during supraglacial lake drainage, Science, 320, 778–781,
831 doi:10.1126/science.1153360, 2008.

832 Davaze, L., Rabatel, A., Dufour, A., Hugonnet, R., and Arnaud, Y.: Region-wide annual glacier surface mass
833 balance for the European Alps from 2000 to 2016, Front. Earth Sci., 8, doi:10.3389/feart.2020.00149, 2020.

834 Delaney, I. and Adhikari, S.: Increased subglacial sediment discharge in a warming climate: consideration of ice
835 dynamics, glacial erosion, and fluvial sediment transport, Geophys. Res. Lett., 47, e2019GL085672,
836 doi:10.1029/2019GL085672, 2020.

837 Dozier, J.: An examination of the variance minimization tendencies of a supraglacial stream, J. Hydrol., 31,
838 359–380, doi:10.1016/0022-1694(76)90134-7, 1976.

839 Edwards, T. L., Nowicki, S., Marzeion, B., Hock, R., Goelzer, H., Seroussi, H., Jourdain, N. C., Slater, D. A.,
840 Turner, F. E., Smith, C. J., McKenna, C. M., Simon, E., Abe-Ouchi, A., Gregory, J. M., Larour, E., Lipscomb, W.
841 H., Payne, A. J., Shepherd, A., Agosta, C., Alexander, P., Albrecht, T., Anderson, B., Asay-Davis, X.,
842 Aschwanden, A., Barthel, A., Bliss, A., Calov, R., Chambers, C., Champollion, N., Choi, Y., Cullather, R.,
843 Cuzzone, J., Dumas, C., Felikson, D., Fettweis, X., Fujita, K., Galton-Fenzi, B. K., Gladstone, R., Golledge, N.
844 R., Greve, R., Hattermann, T., Hoffman, M. J., Humbert, A., Huss, M., Huybrechts, P., Immerzeel, W., Kleiner,

845 T., Kraaijenbrink, P., Le clec'h, S., Lee, V., Leguy, G. R., Little, C. M., Lowry, D. P., Malles, J.-H., Martin, D. F.,
846 Maussion, F., Morlighem, M., O'Neill, J. F., Nias, I., Pattyn, F., Pelle, T., Price, S. F., Quiquet, A., Radić, V.,
847 Reese, R., Rounce, D. R., Rückamp, M., Sakai, A., Shafer, C., Schlegel, N.-J., Shannon, S., Smith, R. S.,
848 Straneo, F., Sun, S., Tarasov, L., Trusel, L. D., Van Breedam, J., van de Wal, R., van den Broeke, M.,
849 Winkelmann, R., Zekollari, H., Zhao, C., Zhang, T., and Zwinger, T.: Projected land ice contributions to twenty-
850 first-century sea level rise, Nature, 593, 74–82, doi:10.1038/s41586-021-03302-y, 2021.

851 Esri. "Imagery" [basemap]. Scale Not Given. "World Imagery". October 10, 2024.
852 https://www.arcgis.com/home/item.html?id=10df2279f9684e4a9f6a7f08febac2a9. (October 22, 2024)

853 Ferguson, R. I.: Sinuosity of supraglacial streams, Geol. Soc. Am. Bull., 84, 251–256, doi:10.1130/0016-
854 7606(1973)84<251:SOSS>2.0.CO;2, 1973.

855 Fischer, M., Huss, M., and Hoelzle, M.: Surface elevation and mass changes of all Swiss glaciers 1980–2010,
856 Cryosphere, 9, 525–540, doi:10.5194/tc-9-525-2015, 2015.

857 Fleischer, F., Otto, J.-C., Junker, R. R., and Hölbling, D.: Evolution of debris cover on glaciers of the Eastern
858 Alps, Austria, between 1996 and 2015, Earth Surf. Process. Landf., 46, 1673–1691, doi:10.1002/esp.5065, 2021.

859 Fyffe, C. L., Brock, B. W., Kirkbride, M. P., Mair, D. W. F., Arnold, N. S., Smiraglia, C., Diolaiuti, G., and
860 Diotri, F.: Do debris-covered glaciers demonstrate distinctive hydrological behaviour compared to clean
861 glaciers?, J. Hydrol., 570, 584–597, doi:10.1016/j.jhydrol.2018.12.069, 2019.

862 Glasser, N. F., Holt, T. O., Evans, Z. D., Davies, B. J., Pelto, M., and Harrison, S.: Recent spatial and temporal
863 variations in debris cover on Patagonian glaciers, Geomorphology, 273, 202–216,
864 doi:10.1016/j.geomorph.2016.07.036, 2016.

865 Gleason, C. J., Smith, L. C., Chu, V. W., Legleiter, C. J., Pitcher, L. H., Overstreet, B. T., Rennermalm, A. K.,
866 Forster, R. R., and Yang, K.: Characterizing supraglacial meltwater channel hydraulics on the Greenland Ice
867 Sheet from in situ observations, Earth Surf. Process. Landf., 41, 2111–2122, doi:10.1002/esp.3977, 2016.

868 Gleason, C. J., Yang, K., Feng, D., Smith, L. C., Liu, K., Pitcher, L. H., Chu, V. W., Cooper, M. G., Overstreet,
869 B. T., Rennermalm, A. K., and Ryan, J. C.: Hourly surface meltwater routing for a Greenlandic supraglacial
870 catchment across hillslopes and through a dense topological channel network, Cryosphere, 15, 2315–2331,
871 doi:10.5194/tc-15-2315-2021, 2021.

872 Gulley, J. D., Benn, D. I., Mueller, D., and Luckman, A.: A cut-and-closure origin for englacial conduits in
873 uncrevassed regions of polythermal glaciers, J. Glaciol., 55, 66–80, doi:10.3189/002214309788608930, 2009.

874 Hambrey, M. J.: Supraglacial drainage and its relationship to structure, with particular reference to Charles
875 Rabots Bre, Okstindan, Norway, Nor. Geogr. Tidsskr., 31, 69–77, doi:10.1080/00291957708545319, 1977.

876 Horton, R. E.: Erosional development of streams and their drainage basins; hydrophysical approach to
877 quantitative morphology, Geol. Soc. Am. Bull., 56, 275–370, doi:10.1130/0016-
878 7606(1945)56[275:EDOSAT]2.0.CO;2, 1945.

879 Hugonnet, R., McNabb, R., Berthier, E., Menounos, B., Nuth, C., Girod, L., Farinotti, D., Huss, M., Dussaillant,
880 I., Brun, F., and Kääb, A.: Accelerated global glacier mass loss in the early twenty-first century, Nature, 592,
881 726–731, doi:10.1038/s41586-021-03436-z, 2021.

882 Huss, M., Bauder, A., Werder, M., Funk, M., and Hock, R.: Glacier-dammed lake outburst events of Gornersee,
883 Switzerland, J. Glaciol., 53, 189–200, doi.org:10.3189/172756507782202784, 2007.

884 Immerzeel, W. W., Lutz, A. F., Andrade, M., Bahl, A., Biemans, H., Bolch, T., Hyde, S., Brumby, S., Davies, B.
885 J., Elmore, A. C., Emmer, A., Feng, M., Fernández, A., Haritashya, U., Kargel, J. S., Koppes, M., Kraaijenbrink,
886 P. D. A., Kulkarni, A. V., Mayewski, P. A., Nepal, S., Pacheco, P., Painter, T. H., Pellicciotti, F., Rajaram, H.,
887 Rupper, S., Sinisalo, A., Shrestha, A. B., Viviroli, D., Wada, Y., Xiao, C., Yao, T., and Baillie, J. E. M.:
888 Importance and vulnerability of the world's water towers, Nature, 577, 364–369, doi:10.1038/s41586-019-1822-
889 y, 2020.

890 Irvine-Fynn, T. D. L., Hodson, A. J., Moorman, B. J., Vatne, G., and Hubbard, A. L.: Polythermal glacier
891 hydrology: a review, Rev. Geophys., 49, doi:10.1029/2010RG000350, 2011.

892 Jobard, S. and Dzikowski, M.: Evolution of glacial flow and drainage during the ablation season, J. Hydrol.,
893 330, 663–671, doi:10.1016/j.jhydrol.2006.04.031, 2006.

894 Karlstrom, L. and Yang, K.: Fluvial supraglacial landscape evolution on the Greenland Ice Sheet, Geophys. Res.
895 Lett., 43, 2683–2692, doi:10.1002/2016GL067697, 2016.

896 Khan, A. L., Xian, P., and Schwarz, J. P.: Black carbon concentrations and modeled smoke deposition fluxes to
897 the bare-ice dark zone of the Greenland Ice Sheet, Cryosphere, 17, 2909–2918, doi:10.5194/tc-17-2909-2023,
898 2023.

899 King, L., Hassan, M. A., Yang, K., and Flowers, G.: Flow routing for delineating supraglacial meltwater channel
900 networks, Remote Sens., 8, 988, doi:10.3390/rs8120988, 2016.

901 Kingslake, J., Ely, J. C., Das, I., and Bell, R. E.: Widespread movement of meltwater onto and across Antarctic
902 ice shelves, Nature, 544, 349–352, doi:10.1038/nature22049, 2017.

903 Knighton, A. D.: Channel form adjustment in supraglacial streams, Austre Okstindbreen, Norway, Arct. Antarct.
904 Alp. Res., 17, 451, doi:10.2307/1550870, 1985.

905 Knighton, A. D.: Channel form and flow characteristics of supraglacial streams, Austre Okstindbreen, Norway,
906 Arct. Alp. Res., 13, 295, doi:10.2307/1551036, 1981.

907 Knighton, A. D.: Meandering habit of supraglacial streams, Geol. Soc. Am. Bull., 83, 201–204,
908 doi:10.1130/0016-7606(1972)83[201:MHOSS]2.0.CO;2, 1972.

909 Leeson, A. A., Shepherd, A., Briggs, K., Howat, I., Fettweis, X., Morlighem, M., and Rignot, E.: Supraglacial
910 lakes on the Greenland Ice Sheet advance inland under warming climate, Nat. Clim. Change, 5, 51–55,
911 doi:10.1038/nclimate2463, 2015.

912 Leidman, S. Z., Rennermalm, Å. K., Muthyala, R., Guo, Q., and Overeem, I.: The presence and widespread
913 distribution of dark sediment in Greenland Ice Sheet supraglacial streams implies substantial impact of
914 microbial communities on sediment deposition and albedo, Geophys. Res. Lett., 48, 2020GL088444,
915 doi:10.1029/2020GL088444, 2021.

916 Leigh, J. R., Stokes, C. R., Carr, R. J., Evans, I. S., Andreassen, L. M., and Evans, D. J. A.: Identifying and
917 mapping very small (<0.5 km^2) mountain glaciers on coarse to high-resolution imagery, J. Glaciol., 65, 873–
918 888, https://doi.org/10.1017/jog.2019.50, 2019.

919 Leinss, S. and Bernhard, P.: TanDEM-X:Deriving InSAR height changes and velocity dynamics of Great
920 Aletsch Glacier, IEEE J. Sel. Top. Appl. Earth Obs. Remote Sens., 14, 4798–4815,
921 https://doi.org/10.1109/JSTARS.2021.3078084, 2021.

922 Linsbauer, A., Huss, M., Hodel, E., Bauder, A., Fischer, M., Weidmann, Y., Bärtschi, H., and Schmassmann, E.:
923 The new Swiss glacier inventory SGI2016: from a topographical to a glaciological dataset, Front. Earth Sci., 9,
924 doi:10.3389/feart.2021.704189, 2021.

925 Mantelli, E., Camporeale, C., and Ridolfi, L.: Supraglacial channel inception: modeling and processes, Water
926 Resour. Res., 51, 7044–7063, doi:10.1002/2015WR017075, 2015.

927 Marston, R. A.: Supraglacial stream dynamics on the Juneau Icefield, Ann. Am. Assoc. Geogr., 73, 597–608,
928 doi:10.1111/j.1467-8306.1983.tb01861.x, 1983.

929 MeteoSwiss: https://www.meteoswiss.admin.ch/, last access: 1 February 2024.

930 Micheletti, N. and Lane, S. N.: Water yield and sediment export in small, partially glaciated Alpine watersheds
931 in a warming climate, Water Resour. Res., 52, 4924–4943, doi: 10.1002/2016WR018774, 2016.

932 Mölg, N., Bolch, T., Walter, A., and Vieli, A.: Unravelling the evolution of Zmuttgletscher and its debris cover
933 since the end of the Little Ice Age, Cryosphere, 13, 1889–1909, doi:10.5194/tc-13-1889-2019, 2019.

934 Moore, R. C.: Origin of Inclosed Meanders on Streams of the Colorado Plateau, J. Glaciol., 34, 29–57,
935 doi:10.1086/623270, 1926.

936 Morriss, B. F., Hawley, R. L., Chipman, J. W., Andrews, L. C., Catania, G. A., Hoffman, M. J., Lüthi, M. P., and
937 Neumann, T. A.: A ten-year record of supraglacial lake evolution and rapid drainage in West Greenland using an
938 automated processing algorithm for multispectral imagery, Cryosphere, 7, 1869–1877, doi:10.5194/tc-7-1869-
939 2013, 2013.

940 Nienow, P., Sharp, M., and Willis, I.: Seasonal changes in the morphology of the subglacial drainage system,
941 Haut Glacier d'Arolla, Switzerland, Earth Surf. Process. Landf., 23, 825–843,
942 https://doi.org/10.1002/(SICI)1096-9837(199809)23:9<825::AID-ESP893>3.0.CO;2-2, 1998.

943 Pitcher, L. H. and Smith, L. C.: Supraglacial Streams and Rivers, Annu. Rev. Earth Planet. Sci., 47, 421–452,
944 doi:10.1146/annurev-earth-053018-060212, 2019.

945 Rippin, D. M., Pomfret, A., and King, N.: High resolution mapping of supra-glacial drainage pathways reveals
946 link between micro-channel drainage density, surface roughness and surface reflectance, Earth Surf. Process.
947 Landf., 40, 1279–1290, doi:10.1002/esp.3719, 2015.

948 Rounce, D. R., Hock, R., Maussion, F., Hugonnet, R., Kochtitzky, W., Huss, M., Berthier, E., Brinkerhoff, D.,
949 Compagno, L., Copland, L., Farinotti, D., Menounos, B., and McNabb, R. W.: Global glacier change in the 21st
950 century: Every increase in temperature matters, Science, 379, 78–83, doi:10.1126/science.abo1324, 2023.

951 Ryan, J. C., Hubbard, A., Stibal, M., Irvine-Fynn, T. D., Cook, J., Smith, L. C., Cameron, K., and Box, J.: Dark
952 zone of the Greenland Ice Sheet controlled by distributed biologically-active impurities, Nat. Commun., 9, 1065,
953 doi:10.1038/s41467-018-03353-2, 2018.

954 Seaberg, S. Z., Seaberg, J. Z., Hooke, R. L., and Wiberg, D. W.: Character of the englacial and subglacial
955 drainage system in the lower part of the ablation area of Storglaciären, Sweden, as Revealed by Dye-Trace
956 Studies, J. Glaciol., 34, 217–227, doi:10.3189/S0022143000032263, 1988.

957 Shepherd, R. G.: Incised river meanders: evolution in simulated bedrock, Science, 178, 409–411,
958 doi:10.1126/science.178.4059.409, 1972.

959 Smith, L. C., Chu, V. W., Yang, K., Gleason, C. J., Pitcher, L. H., Rennermalm, A. K., Legleiter, C. J., Behar, A.
960 E., Overstreet, B. T., Moustafa, S. E., Tedesco, M., Forster, R. R., LeWinter, A. L., Finnegan, D. C., Sheng, Y.,
961 and Balog, J.: Efficient meltwater drainage through supraglacial streams and rivers on the southwest Greenland
962 Ice Sheet, Proc. Natl. Acad. Sci., 112, 1001–1006, doi:10.1073/pnas.1413024112, 2015.

963 Sommer, C., Malz, P., Seehaus, T. C., Lippl, S., Zemp, M., and Braun, M. H.: Rapid glacier retreat and
964 downwasting throughout the European Alps in the early 21st century, Nat. Commun., 11, 3209,
965 doi:10.1038/s41467-020-16818-0, 2020.

966 St Germain, S. L. and Moorman, B. J.: Long-term observations of supraglacial streams on an Arctic glacier, J.
967 Glaciol., 65, 900–911, doi:10.1017/jog.2019.60, 2019.

968 Swift, D. A., Nienow, P. W., Spedding, N., and Hoey, T. B.: Geomorphic implications of subglacial drainage
969 configuration: rates of basal sediment evacuation controlled by seasonal drainage system evolution, Sediment.
970 Geol., 149, 5–19, doi:10.1016/S0037-0738(01)00241-X, 2002.

971 Tepes, P., Gourmelen, N., Nienow, P., Tsamados, M., Shepherd, A., and Weissgerber, F.: Changes in elevation
972 and mass of Arctic glaciers and ice caps, 2010–2017, Remote Sens. Environ., 261, 112481,
973 doi:10.1016/j.rse.2021.112481, 2021.

974 The GlaMBIE Team: Community estimate of global glacier mass changes from 2000 to 2023, Nature, 1–7,
975 doi:10.1038/s41586-024-08545-z, 2025.

976 ~~Turowski, J. M.: Alluvial cover controlling the width, slope and sinuosity of bedrock channels, Earth Surf. Dyn.,~~
977 ~~6, 29–48, doi:10.5194/esurf-6-29-2018, 2018.~~

978 Willis, I.C.: Intra-annual variations in glacier motion: a review, Prog. Phys. Geogr., 19.
979 doi:10.1177/030913339501900104, 1995.

980 Wouters, B., Gardner, A. S., and Moholdt, G.: Global glacier mass loss during the GRACE satellite mission
981 (2002-2016), Front. Earth Sci., 7, 2019.

982 Yang, K. and Smith, L. C.: Internally drained catchments dominate supraglacial hydrology of the southwest
983 Greenland Ice Sheet, J. Geophys. Res.-Earth Surf., 121, doi:10.1002/2016JF003927, 2016.

984 Yang, K. and Smith, L. C.: Supraglacial streams on the Greenland Ice Sheet delineated from combined spectral-
985 shape information in high-resolution satellite imagery, IEEE Geosci. Remote Sens. Lett., 10, 801–805,
986 doi:10.1109/LGRS.2012.2224316, 2013.

987 Yang, K., Smith, L. C., Andrews, L. C., Fettweis, X., and Li, M.: Supraglacial drainage efficiency of the
988 Greenland Ice Sheet estimated from remote sensing and climate models, J. Geophys. Res.-Earth Surf., 127,
989 e2021JF006269, doi:10.1029/2021JF006269, 2022.

990 Yang, K., Smith, L. C., Chu, V. W., Gleason, C. J., and Li, M.: A caution on the use of surface digital elevation
991 models to simulate supraglacial hydrology of the Greenland Ice Sheet, IEEE J. Sel. Top. Appl. Earth Observ.
992 Remote Sens., 8, 5212–5224, doi:10.1109/JSTARS.2015.2483483, 2015.

993 Yang, K., Smith, L. C., Chu, V. W., Pitcher, L. H., Gleason, C. J., Rennermalm, A. K., and Li, M.: Fluvial
994 morphometry of supraglacial river networks on the southwest Greenland Ice Sheet, GISci. Remote Sens., 53,
995 459–482, doi:10.1080/15481603.2016.1162345, 2016.

996 Yang, K., Smith, L. C., Cooper, M. G., Pitcher, L. H., As, D. van, Lu, Y., Lu, X., and Li, M.: Seasonal evolution
997 of supraglacial lakes and rivers on the southwest Greenland Ice Sheet, J. Glaciol., 67, 592–602,
998 doi:10.1017/jog.2021.10, 2021.

999 Yang, K., Smith, L. C., Karlstrom, L., Cooper, M. G., Tedesco, M., van As, D., Cheng, X., Chen, Z., and Li, M.:
1000 A new surface meltwater routing model for use on the Greenland Ice Sheet surface, Cryosphere, 12, 3791–3811,
1001 doi:10.5194/tc-12-3791-2018, 2018.

1002 Yang, K., Smith, L. C., Sole, A., Livingstone, S. J., Cheng, X., Chen, Z., and Li, M.: Supraglacial rivers on the
1003 northwest Greenland Ice Sheet, Devon Ice Cap, and Barnes Ice Cap mapped using Sentinel-2 imagery, Int. J.
1004 Appl. Earth Obs. Geoinf., 78, 1–13, doi:10.1016/j.jag.2019.01.008, 2019.

1005 Yang, K., Sommers, A., Andrews, L. C., Smith, L. C., Lu, X., Fettweis, X., and Li, M.: Intercomparison of
1006 surface meltwater routing models for the Greenland Ice Sheet and influence on subglacial effective pressures,
1007 Cryosphere, 14, 3349–3365, doi:10.5194/tc-14-3349-2020, 2020.

1008 Zekollari, H., Huss, M., and Farinotti, D.: Modelling the future evolution of glaciers in the European Alps under
1009 the EURO-CORDEX RCM ensemble, Cryosphere, 13, 1125–1146, doi:10.5194/tc-13-1125-2019, 2019.

1010 Zemp, M., Huss, M., Thibert, E., Eckert, N., McNabb, R., Huber, J., Barandun, M., Machguth, H., Nussbaumer,
1011 S. U., Gärtner-Roer, I., Thomson, L., Paul, F., Maussion, F., Kutuzov, S., and Cogley, J. G.: Global glacier mass
1012 changes and their contributions to sea-level rise from 1961 to 2016, Nature, 568, 382–386, doi:10.1038/s41586-
1013 019-1071-0, 2019.